AD-A169 350 FORCED OSCILLATION OF A TWO-DIMENSIONAL AIRFOIL WITH NONLINEAR AERODYNAMI..(U) NATIONAL AERONAUTICAL ESTABLISHMENT OTTAWA (ONTARIO) B H LEE ET AL. JAN 86 1/1

UNCLASSIFIED NAE-LR-617 NRC-25411 F/G 20/4 NL

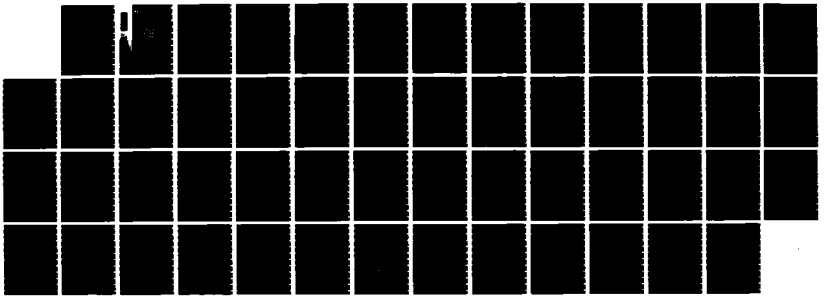

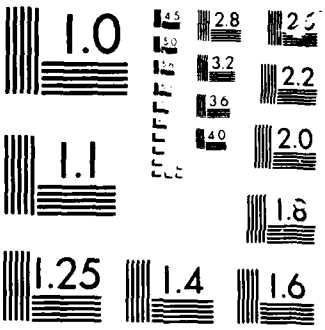
1.0
1.1
1.25
1.4
1.6
2.8
3.2
3.6
4.0
2.2
2.0
1.8

National Research Council Canada
Conseil national de recherches Canada

FORCED OSCILLATION OF A TWO-DIMENSIONAL AIRFOIL WITH NONLINEAR AERODYNAMIC LOADS

by

B.H.K. Lee, P. LeBlanc

National Aeronautical Establishment

OTTAWA
JANUARY 1986

AERONAUTICAL REPORT
LR-617
NRC NO. 25411

NATIONAL AERONAUTICAL ESTABLISHMENT

SCIENTIFIC AND TECHNICAL PUBLICATIONS

AERONAUTICAL REPORTS:

Aeronautical Reports (LR): Scientific and technical information pertaining to aeronautics considered important, complete, and a lasting contribution to existing knowledge.

Mechanical Engineering Reports (MS): Scientific and technical information pertaining to investigations outside aeronautics considered important, complete, and a lasting contribution to existing knowledge.

AERONAUTICAL NOTES (AN): Information less broad in scope but nevertheless of importance as a contribution to existing knowledge.

LABORATORY TECHNICAL REPORTS (LTR): Information receiving limited distribution because of preliminary data, security classification, proprietary, or other reasons.

Details on the availability of these publications may be obtained from:

Publications Section,
National Research Council Canada,
National Aeronautical Establishment,
Bldg. M-16, Room 204,
Montreal Road,
Ottawa, Ontario
K1A 0R6

ÉTABLISSEMENT AÉRONAUTIQUE NATIONAL

PUBLICATIONS SCIENTIFIQUES ET TECHNIQUES

RAPPORTS D'AÉRONAUTIQUE

Rapports d'aéronautique (LR): Informations scientifiques et techniques touchant l'aéronautique jugées importantes, complètes et durables en termes de contribution aux connaissances actuelles.

Rapports de génie mécanique (MS): Informations scientifiques et techniques sur la recherche externe à l'aéronautique jugées importantes, complètes et durables en termes de contribution aux connaissances actuelles.

CAHIERS D'AÉRONAUTIQUE (AN): Informations de moindre portée mais importantes en termes d'accroissement des connaissances.

RAPPORTS TECHNIQUES DE LABORATOIRE (LTR): Informations peu disséminées pour des raisons d'usage secret, de droit de propriété ou autres ou parce qu'elles constituent des données préliminaires.

Les publications ci-dessus peuvent être obtenues à l'adresse suivante:

Section des publications
Conseil national de recherches Canada
Établissement aéronautique national
Im. M-16, pièce 204
Chemin de Montréal
Ottawa (Ontario)
K1A 0R6

FORCED OSCILLATION OF A TWO-DIMENSIONAL AIRFOIL WITH NONLINEAR AERODYNAMIC LOADS

OSCILLATION FORCÉE D'UN PROFIL DE VOILURE BIDIMENSIONNEL SOUS DES CHARGES AÉRODYNAMIQUES NON LINÉAIRES

by/par

B.H.K. Lee, P. LeBlanc*

*Co-op Student, University of Waterloo

L.H. Ohman, Head/Chef
High Speed Aerodynamics Laboratory/
Laboratoire d'aérodynamique à hautes vitesses

G.M. Lindberg
Director/Directeur

$$K = \frac{4x_\alpha}{\Delta\tau^2}$$

$$L = \frac{x_\alpha}{\Delta\tau^2}$$

$$N = \frac{5}{\Delta\tau^2} + \frac{6}{\Delta\tau}\zeta_\xi\frac{\bar{\omega}}{U^*}$$

$$P = \frac{4}{\Delta\tau^2} + \frac{3}{\Delta\tau}\zeta_\xi\frac{\bar{\omega}}{U^*}$$

$$S = \frac{1}{\Delta\tau^2} + \frac{2}{3\Delta\tau}\zeta_\xi\frac{\bar{\omega}}{U^*}$$

and

$$E = \frac{2x_\alpha}{r_\alpha^2\Delta\tau^2} \tag{A3}$$

$$V = \frac{2}{\Delta\tau^2} + \frac{11}{3\Delta\tau}\frac{\zeta_\alpha}{U^*} + \frac{1}{U^{*2}} \tag{A4}$$

$$M = \frac{2}{\Delta\tau^2} + \frac{11}{3\Delta\tau}\zeta_\xi\frac{\bar{\omega}}{U^*} + \frac{\bar{\omega}^2}{U^{*2}} \tag{A5}$$

$$I = \frac{2x_\alpha}{\Delta\tau^2} \tag{A6}$$

SUMMARY

Forced oscillation of a two-dimensional airfoil with attached and separated flows is investigated using nonlinear unsteady aerodynamics for pitching motion derived from a time synthesization technique utilizing oscillatory loop data determined experimentally. Both one- and two-degree-of-freedom oscillations are considered. The structural dynamic equations of motion are integrated by a time marching finite difference scheme. The airfoil response is examined for different values of spring stiffness and magnitudes of externally applied moment. For two-degree-of-freedom vibration, only small plunge amplitude is considered and the aerodynamic loads are approximated by the superposition of nonlinear terms due to pitch and linear terms due to plunge. The presence of a small amplitude plunging motion increases the pitch amplitude slightly for attached flow, while a decrease in pitch amplitude is predicted for separated flow.

RÉSUMÉ

On examine l'oscillation forcée d'un profil de voilure bidimensionel dans des écoulements de contact et séparé à partir de données d'aérodynamique non linéaire instable sur le mouvement de tangage produites par une technique de synthétisation du temps basée sur une boucle oscillatoire établie expérimentalement. On étudie les oscillations à un et à deux degrés de liberté. Les équations dynamiques structurales du mouvement sont intégrées par une méthode d'avancement du temps aux différences finies. La réponse du profil est examinée pour différentes valeurs de raideur d'un ressort et de moment externe. Pour les vibrations à deux degrés de liberté, seule l'amplitude des faibles plongeons est considérée et les charges aérodynamiques sont approchées par la superposition de termes non linéaires de tangage et de termes linéaires de plongeon. La présence d'un mouvement de plongeon de faible amplitude augmente légèrement l'amplitude du tangage pour l'écoulement de contact, tandis qu'on prévoit une diminution de l'amplitude du tangage pour l'écoulement séparé.

TABLE OF CONTENTS

ILLUSTRATIONS

ILLUSTRATIONS (Cont'd)

ILLUSTRATIONS (Cont'd)

SYMBOLS

Symbol	Definition
A	pitch rate
A_{Dm}	pitch rate at dynamic stall
a_h	non-dimensional distance measured from airfoil mid-chord to elastic axis
a_{o_M}	aerodynamic sectional static pitching moment slope at zero angle-of-attack
a_{o_N}	aerodynamic sectional static normal force curve slope
b	semi-chord of airfoil
C_M	sectional aerodynamic pitching moment coefficient
C_{M_S}	sectional aerodynamic static pitching moment coefficient
C_{Am}, C_{Wm}	empirical constants in Equation (4)
C_{AR}, C_{WR}	empirical constants in Equation (5)
C_{At}, $C_{\alpha t}$	empirical constants in Equation (6)
C_N	sectional aerodynamic normal force coefficient
C_{N_S}	sectional aerodynamic static force coefficient
c	chord
f_α	natural frequency of pitch oscillation
h	plunge displacement
k	reduced frequency, $\omega b/U$
M	free stream Mach number
m	mass of airfoil per unit span
P	external applied force

SYMBOLS (Cont'd)

Symbol	Definition
$P_1 \ldots P_{10}$	empirical coefficients in Equation 7
Q	external applied moment
Q_o	amplitude of external applied moment
$Q_1 \ldots Q_7$	empirical constants in Equation 13
R_e	Reynolds number
r_α	radius of gyration about elastic axis
t	time
t_{dm}	time when dynamic stall occurs
U	free stream velocity
U^*	defined in Equation 17
x_α	non-dimensional distance measured from elastic axis to centre of mass
α	pitch angle
α_{Dm}	angle of attack at dynamic stall
α_m	mean angle of attack
α_{RE}	angle of attack at reattachment
α_{SS}	angle of attack at static stall
α_{TE}	angle of attack when vortex leaves trailing edge
α_W	defined in Equation (1)
α_{Wm}	value of α_W at dynamic stall
β	$\sqrt{1-M^2}$
β_1	empirical constant taken as 0.18
δ_1	defined in Equation (11)
δ_2	defined in Equation (12)
ϵ	empirical constant
ζ_α	viscous damping for pitching motion

SYMBOLS (Cont'd)

Symbol	Definition
ζ_ξ	viscous damping for plunging motion
μ	airfoil-air mass ratio , = $m/\pi\rho b^2$
ξ	non-dimensional displacement
ρ	air density
τ	non-dimensional time
τ_m	non-dimensional time measured from instant of stall onset
τ_{mt}	defined in Equation (6)
ϕ_α	phase angle of pitch oscillation
ϕ_c	defined in Equation (3)
ω	frequency
ω_ξ	uncoupled natural frequency of plunging motion
ω_α	uncoupled natural frequency of pitching motion
$\bar{\omega}$	ratio ω_ξ/ω_α
Subscripts	
o	initial conditions

FORCED OSCILLATION OF A TWO-DIMENSIONAL AIRFOIL WITH NONLINEAR AERODYNAMIC LOADS

1.0 INTRODUCTION

The dynamic response of a two-dimensional airfoil to external oscillatory forces or moments using linear aerodynamic loads derived from incompressible flow is a well known subject (Refs. 1, 2). For more complex aerodynamics as in transonic flow, numerical time marching techniques have been used. The first study was reported by Ballhaus and Goorjian (Ref. 3) who carried out the aeroelastic response of a NACA64A006 airfoil with a single-degree-of-freedom in pitch at transonic speeds. Extensions of this procedure to two- and three-degree-of-freedom have been reported by Rizzetta (Ref. 4) and Yang and Chen (Ref. 5). Only a linear response was treated by these authors.

In aeroelastic studies, there are potentially many sources of nonlinearities present, but the most commonly encountered ones are those having structural or aerodynamic origin. Existing techniques of analysing dynamic response based on linear vibration theory are not applicable. Numerical methods are the obvious choice in solving non-linear vibration problems since they do not suffer from the limitations of perturbation theory. However, they have received little attention until recently, and this study shows the usefulness of the numerical approach in dealing with aerodynamic nonlinearities associated with stalled and unstalled airfoils. This problem has hitherto not been amenable to theoretical analysis. A prediction method of the dynamic response is useful in providing information on the sequence of events occurring on the airfoil during a cycle of oscillation. There are many applications for such a method, for example, in wind tunnel tests of oscillating airfoils at high incidence or large amplitude oscillations. In helicopter rotor blades design, the method can predict unsteady airloads and deflections of the blades in forward flights or manoeuvring operations.

There exists a number of numerical time marching techniques developed for finite element linear structural analysis. Among the most commonly used time integration schemes are the explicit central difference technique and Houbolt's, Wilson's and Newmark's methods (Refs. 6, 7). Except for the explicit scheme, the other three methods are unconditionally stable. Higher order schemes are also discussed in Reference 8 and they are conditionally stable. Provided that care is taken to choose a time step sufficiently small to ensure the highest mode considered in a vibrating system does not diverge, higher order schemes are more efficient in terms of computation time. However, for a system with few structural components or the number of vibration modes is small, higher order methods such as the eighth order scheme reported in Reference 8 does not offer any distinct advantage over Houbolt's scheme which is simpler and less cumbersome to use.

The use of numerical time integration techniques to study nonlinear vibration in one-degree-of-freedom was reported in Reference 8. The nonlinearities considered was that of a cubic spr[illegible].σ. The numerical results agree very well with analytical predictions derived from perturbation theory, and in addition, give more information on the behaviour of the system to initial conditions which the analytical method fails to provide.

In this study, Houbolt's (Ref. 7) scheme is used to investigate the forced oscillation of an airfoil in one- and two-degree-of-freedom. For the one-degree-of-freedom motion case, only pitch oscillation is investigated and both stalled and unstalled flow are considered. There are a number of studies (Refs. 9-14) on methods of predicting dynamic stall and unsteady airloads on two-dimensional airfoils with harmonic pitching motion. The most sophisticated one is given by Bielawa et al. (Ref. 14) using experimental oscillatory loop data to generate synthesized data in the time domain. This method is used in the present study since it conveniently generates the aerodynamic loads at each time step in the integration of the structural dynamic equations of motion.

In the two-degree-of-freedom vibration of the airfoil, the plunge amplitude is assumed to be small. The aerodynamic loads are then approximated by the superposition of nonlinear terms due to pitch and linear terms due to plunge, since empirical relations for both large amplitude pitch and

plunge motions are not available. A comparison with one-degree-of-freedom response results gives the effect of a small plunging motion for cases with attached or separated flow on the airfoil.

2.0 ANALYSIS

2.1 Empirical Representation of Unsteady Aerodynamic Loads of Stalled and Unstalled Airfoils

In Reference 14 an empirical method to determine the aerodynamic loads is given in the time-domain using data obtained from oscillating airfoil experiments. The expressions for the normal force and pitching moment coefficients are quite general and valid for both stalled and unstalled airfoils. For a given airfoil shape, Mach number and Reynolds number, the dynamic characteristics of the airfoil depend on the mean angle of attack, the frequency and amplitude of oscillations. In the case of dynamic stall, it is assumed that a vortex develops near the leading edge when the static stall angle is exceeded. As the angle of incidence α increases, the vortex detaches from the leading edge and convects downstream near the surface until it leaves the trailing edge. The airfoil remains stalled until α drops significantly for reattachment of flow to occur.

Bielawa et al. (Ref. 14) define a parameter α_W which accounts for the time history effects of the change in α and is given by

$$\alpha_W(\tau) = \alpha(\tau) - \alpha(0)\beta\,\phi_c(\tau,M) - \int_0^\tau \frac{d\alpha}{d\tau}\,\beta\,\phi_c(\tau-\sigma,M)\,d\sigma \tag{1}$$

where τ is the non-dimensional time

$$\tau = \frac{Ut}{b} \tag{2}$$

$\beta = \sqrt{1-M^2}$, $\alpha(0)$ is the initial angle of attack at time $\tau = 0$, and $\phi_c(\tau,M)$ is the compressibility corrected Wagner function which is written as

$$\phi_c(\tau,M) = \frac{1}{\beta}\left\{1 - 0.165e^{-0.0455\,\tau\beta^2} - 0.335e^{-0.3\,\tau\beta^2}\right\} \tag{3}$$

The equations in the rest of this section are essentially the same as those obtained from Reference 14. They are included here since they are used in the numerical finite difference scheme to be described in the next section. For a detailed description of the time synthesization technique, the derivation given by Bielawa (Ref. 14) should be referred to.

The dynamic stall and reattachment angles in terms of the static stall angle α_{SS}, the pitch rate A and α_W are defined as

$$\alpha_{Dm} = (1 + \epsilon + C_{Am}\,A_{Dm} + C_{Wm}\,\alpha_{Wm})\alpha_{SS} \tag{4}$$

and

$$\alpha_{RI} = (1 - \epsilon + C_{AR}\,A_{Dm} + C_{WR}\,\alpha_{Wm})\alpha_{SS} \tag{5}$$

where ϵ, C_{Am}, C_{Wm}, C_{AR} and C_{WR} are empirical constants to be determined. The following relationship is used to predict the time it takes for the vortex to travel from the leading edge to the trailing edge of the airfoil:

$$\tau_{mt} = \frac{1}{C_{At}\, A_{Dm} + C_{\alpha t}\, \alpha_{Dm}} \tag{6}$$

where C_{At} and $C_{\alpha t}$ are empirical constants. The normal force coefficient is given as

$$C_N = C_{N_S}\,(\alpha - \Delta\alpha_1 - \Delta\alpha_2) + a_{o_L}\,\Delta\alpha_1 + P_4 A + P_5\alpha_W$$

$$+ P_6\left(\frac{\alpha}{\alpha_{SS}}\right) + P_7\left(\frac{\alpha}{\alpha_{SS}}\right)^2 + P_8\,\delta_1 + P_9\,\Delta\alpha_2$$

$$+ P_{10}\,\alpha_{Dm}{}^2\left[\frac{1 - e^{-(\beta_1\tau_m)^3}}{(\beta_1\tau_m)^2}\right] \tag{7}$$

where

$$\Delta\alpha_1 = (P_1 A + P_2\alpha_W + P_3)\alpha_{SS} \tag{8}$$

$$\Delta\alpha_2 = \delta_2\,\alpha_{SS} \tag{9}$$

$$\tau_m = \frac{2U(t - t_{dm})}{c} \tag{10}$$

P_1 to P_{10} are empirical constants, a_{o_L} is the static lift curve slope, β_1 is an empirical constant taken to be 0.18, and t_{dm} is the time when dynamic stall first occurs. δ_1 and δ_2 are defined by the following

$$\delta_1 = \begin{cases} 0 & \alpha \leqslant \alpha_{SS} \\ \dfrac{\alpha}{\alpha_{SS}} - 1 & \alpha_{SS} \leqslant \alpha \leqslant \alpha_{Dm} \\ \left(\dfrac{\alpha_{Dm}}{\alpha_{SS}} - 1\right)\left[1 - \left(\dfrac{\tau_m}{\tau_{mt}}\right)^2\right] & 0 \leqslant \tau_m \leqslant \tau_{mt} \\ 0 & \tau_m > \tau_{mt} \end{cases} \tag{11}$$

$$\delta_2 = \begin{cases} 0 & \alpha \leqslant \alpha_{SS} \\ \dfrac{\alpha}{\alpha_{SS}} - 1 & \alpha_{SS} \leqslant \alpha \leqslant \alpha_{Dm} \\ \dfrac{\alpha_{Dm}}{\alpha_{SS}} - 1 & 0 \leqslant \tau_m \leqslant \tau_{mt} \\ \left(\dfrac{\alpha_{Dm}}{\alpha_{SS}} - 1\right)\left(\dfrac{\alpha - \alpha_{RE}}{\alpha_{TE} - \alpha_{RE}}\right) & \alpha_{RE} \leqslant \alpha \leqslant \alpha_{TE} \\ 0 & \alpha \leqslant \alpha_{RE} \end{cases} \tag{12}$$

The pitching coefficient is expressed as

$$C_M = C_{M_S}(\alpha - \Delta\alpha_2) + a_{o_M}\Delta\alpha_2 + Q_1 A + Q_2 \alpha_W + Q_3\left(\frac{\alpha}{\alpha_{SS}}\right)$$

$$+ Q_4 |\alpha_W| + Q_5 \delta_1 + Q_6 \Delta\alpha_2 + Q_7 \alpha_{Dm} A_{Dm} \tau_m \tag{13}$$

where a_{o_M} is the static pitching moment slope at zero angle of attack. For unstalled airfoils, the last three terms in Equation (13) are zero.

2.2 Two-Degree-of-Freedom Motion of a 2-D Airfoil

Figure 1 shows the notations used in the analysis of a two-degree-of-freedom motion of an airfoil oscillating in pitch and in plunge. The plunging deflection is denoted by h, positive in the downward direction. α is the pitch angle about the elastic axis, positive with the nose up. The elastic axis is located at a distance $a_h b$ from the midchord, while the mass centre is located at a distance $x_\alpha b$ from the elastic axis. Both distances are positive when measured towards the trailing edge of the airfoil. The aeroelastic equations of motion have been derived by Fung (Ref. 2) and can be written as

$$\ddot{\xi} + x_\alpha \ddot{\alpha} + 2\zeta_\xi \frac{\bar{\omega}}{U^*}\dot{\xi} + \frac{\bar{\omega}^2}{U^{*2}}\xi = -\frac{1}{\pi\mu} C_N(\tau) + \frac{P(\tau)b}{mU^2} \tag{14}$$

$$x_\alpha \ddot{\xi} + r_\alpha^2 \ddot{\alpha} + r_\alpha^2 2\zeta_\alpha \frac{\dot{\alpha}}{U^*} + \frac{r_\alpha^2}{U^{*2}}\alpha = \frac{2}{\pi\mu} C_M(\tau) + \frac{Q(\tau)}{mU^2} \tag{15}$$

where $\xi = h/b$ is the non-dimensional displacement, m is the mass per unit span of the airfoil and

$$\bar{\omega} = \omega_\xi / \omega_\alpha \tag{16}$$

ω_ξ, ω_α are the uncoupled plunging and pitching natural frequency respectively, ζ_ξ and ζ_α are the viscous damping ratio for plunge and pitch motion respectively, r_α is the radius of gyration about the elastic axis, C_N and C_M are the normal force and pitching moment coefficients, and $P(\tau)$ and $Q(\tau)$ are the external applied force and moment respectively. U* is defined as

$$U^* = \frac{U}{b\omega_\alpha} \tag{17}$$

For given $P(\tau)$ and/or $Q(\tau)$, Equations (14) and (15) can be solved for the forced oscillation of the airfoil in pitch and plunge provided that $C_N(\tau)$ and $C_M(\tau)$ are known. In linear analysis for small oscillations of the airfoil, superposition of C_N and C_M for pitch and plunge motions is permissible in determining the total force and moment coefficients. However, when the aerodynamic loads are nonlinear, these coefficients have to be determined for combined motions in pitch and plunge. The two-degree-of-freedom oscillating airfoil studied in this report has large stiffness in the plunge motion. In the limit when $\bar{\omega}$ is infinite, the motion degenerates to that of a one-degree-of-freedom system. Since the plunging motion is assumed to be small, the values of C_N and C_M are predominantly due to pitching motion. The contributions due to plunge are added on from linear aerodynamic theory and hence they should be treated as corrections which are only approximations to an otherwise extremely complex situation.

2.3 Finite Difference Scheme

Houbolt's (Ref. 7) implicit method is used in the present analysis even though more accurate higher order schemes are available (Ref. 8). In this case, the derivatives at time $\tau + \Delta\tau$ are replaced with backward difference formulas using values at three previous points. For example,

$$\ddot{\alpha}_{\tau+\Delta\tau} = \frac{1}{\Delta\tau^2}\left(2\alpha_{\tau+\Delta\tau} - 5\alpha_\tau + 4\alpha_{\tau-\Delta\tau} - \alpha_{\tau-2\Delta\tau}\right) + (\Delta\tau^2) \tag{18}$$

and

$$\dot{\alpha}_{\tau+\Delta\tau} = \frac{1}{6\Delta\tau}\left(11\alpha_{\tau+\Delta\tau} - 18\alpha_\tau + 9\alpha_{\tau-\Delta\tau} - 2\alpha_{\tau-2\Delta\tau}\right) + 0(\Delta\tau^3) \tag{19}$$

Similar expressions can be written for $\ddot{\xi}_{\tau+\Delta\tau}$ and $\dot{\xi}_{\tau+\Delta\tau}$. In difference form, Equations (14) and (15) can be written as

$$E\,\xi_{\tau+\Delta\tau} + V\alpha_{\tau+\Delta\tau} = T \tag{20}$$

$$M\,\xi_{\tau+\Delta\tau} + I\alpha_{\tau+\Delta\tau} = U \tag{21}$$

The coefficients E, V, M, I and the terms T and U on the RHS of Equations (20) and (21) are given in the Appendix.

2.4 Starting Procedure

Houbolt's scheme requires values of α and ξ at times $\tau-2\Delta\tau$, $\tau-\Delta\tau$ and τ in order to determine their values at $\tau+\Delta\tau$. At time $\tau = 0$ a special starting procedure is required. Writing Equations (14) and (15) at $\tau = 0$ and solving for $\ddot{\alpha}_0$ and $\ddot{\xi}_0$ gives

$$\ddot{\alpha}_o = \frac{\frac{x_\alpha}{r_\alpha^2}\left(p_o - 2\zeta_\xi \frac{\bar{\omega}}{U^*}\dot{\xi}_o - \frac{\bar{\omega}^2}{U^{*2}}\xi_o\right) - \left(r_o - 2\zeta_\alpha \frac{\dot{\alpha}_o}{U^*} - \frac{\alpha_o}{U^{*2}}\right)}{\frac{x_\alpha^2}{r_\alpha^2} - 1} \tag{22}$$

$$\ddot{\xi}_o = \frac{\frac{x_\alpha}{r_\alpha^2}\left(r_o - 2\zeta_\alpha \frac{\dot{\alpha}_o}{U^*} - \frac{\alpha_o}{U^{*2}}\right) - \left(p_o - 2\zeta_\xi \frac{\bar{\omega}}{U^*}\dot{\xi}_o - \frac{\bar{\omega}^2}{U^{*2}}\xi_o\right)}{\frac{x_\alpha^2}{r_\alpha^2} - 1} \tag{23}$$

where p_o and r_o can be obtained from the Appendix, and the initial conditions α_o, $\dot{\alpha}_o$, ξ_o and $\dot{\xi}_o$ are known. A Taylor series is then used to obtain the following

$$\alpha_{-\Delta\tau} = \alpha_o - \Delta\tau\,\dot{\alpha}_o + \frac{\Delta\tau^2}{2}\ddot{\alpha}_o + 0(\Delta\tau^3) \tag{24}$$

$$\alpha_{\Delta\tau} = \alpha_o + \Delta\tau\,\dot{\alpha}_o + \frac{\Delta\tau^2}{2}\ddot{\alpha}_o + 0(\Delta\tau^3) \tag{25}$$

with similar expressions for $\xi_{-\Delta\tau}$ and $\xi_{\Delta\tau}$. For the next step, Houbolt's scheme can be used since $\alpha_{-\Delta\tau}$, α_o, $\alpha_{\Delta\tau}$, $\xi_{-\Delta\tau}$, ξ_o and $\xi_{\Delta\tau}$ are known. The accuracy of the numerical method is $0(\Delta\tau^4)$ on each step while Equations (24) and (25) limit the accuracy to $0(\Delta\tau^3)$. A starting accuracy higher than $0(\Delta\tau^3)$ is not necessary since the error per cycle in the numerical scheme is $\frac{2\pi}{\omega}\,0(\Delta\tau^3)$ (Ref. 8).

3.0 RESULTS AND DISCUSSIONS

3.1 Synthesized Data for a Vertol Modified NACA0012 Airfoil

In Reference 15 two-dimensional oscillatory airfoil test data sets for pitching motion are given for a Vertol Modified NACA0012 airfoil. In this report the synthesized data are only shown for M = 0.6 and $R_e = 6.2 \times 10^6$. Equations (4) to (6) predict the stall events and the coefficients in these equations are determined empirically. The force and moment coefficients are obtained from Equations (7) and (13) by a curve fitting procedure using data loops for both unstalled and stalled conditions. In this particular example, 13 data loops are used for C_N and 14 data loops for C_M. The coefficients in the two equations are obtained by a minimization procedure given by Powell (Ref. 16). Usually in each cycle of oscillation of the airfoil, the loop is divided into 600 time steps. The steps are adjusted so that the spacings are reduced in regions where large changes in aerodynamic characteristics occur.

In Table 1, the empirical coefficients in Equations (4) to (6) and those for C_N and C_M at M = 0.62 and $R_e = 6.2 \times 10^6$ are given. The comparisons between the synthesized and test data are shown in Figures 2 and 3. The correlation is very similar to that obtained by Bielawa et al. (Ref. 14) which is considered to be good compared to other empirical formulations.

3.2 Forced Oscillation for Pitching Motions

For very large values of $\bar{\omega}$, Equations (14) and (15) reduce to that for pitch oscillation. The forcing function in Equation (15), that is, $Q(\tau)/mU^2$ can be written as $Q_0 \sin k\tau$ where the reduced frequency $k = \omega b/U$.

Figure 4a shows the angular displacement from the mean, C_N and C_M for the first five cycles after an external moment has been applied at $\tau = 0$. The pitch axis is at the 1/4 chord, and the mean angle of attack α_m is 0.2°. The initial displacement and angular velocity of the airfoil are zero. The driving frequency corresponds to that for a value of $k = 0.165$. The amplitude of the applied moment is $Q_0 = 0.8 \times 10^{-3}$, $\zeta_\alpha = 0$ and $\omega/\omega_\alpha = 0.9$. The airfoil has the following properties: $\mu = 100$, $r_\alpha = 0.5$, $x_\alpha = 0.25$ and $a_h = -0.5$. The flow around the airfoil is attached at all times and the oscillations reach a steady states in four or five cycles. The results between 15 to 20 cycles are shown in Figure 4b and it is seen that they are practically the same as those at the fifth cycle. In all computations, a time step equal to 1/128 of a cycle is used and found to give sufficiently accurate results.

At larger mean angle of attack when the airfoil stalls, it usually takes a few more cycles before a steady state is reached. Figures 5a and 5b show the first five and the 15 to 20 cycles for $\alpha_m = 7.48°$, $Q_0 = 0.5 \times 10^{-3}$, $\omega/\omega_\alpha = 1.4$ and $k = 0.165$.

Figures 6 and 7 show the amplitude and phase of an unstalled airfoil at $\alpha_m = 0.2°$, $M = 0.6$ for three values of Q_0. The driving frequency is kept constant at a value of $k = 0.165$, and varying ω/ω_α is equivalent to changing the stiffness of the torsional spring constant. Since $\zeta_\alpha = 0$, the damping is solely from the aerodynamics. The phase curves for $Q_0 = 0.5$ and 0.8×10^{-3} are shifted upward by 20°. These two figures are very similar to those for one-degree-of-freedom system with viscous damping.

With the same value of k but increasing α_m to 7.48°, the amplitude and phase curves are shown in Figures 8 and 9 for six values of the amplitude of the external driving moment Q_0. Again, the phase curves are shifted upwards by 20°. Except for curve '6' with the smallest value of $Q_0 = 0.1 \times 10^{-3}$, the other five cases exhibit breaks in the amplitude and phase versus ω/ω_α curves. Starting with small values of ω/ω_α, the flow over the airfoil is attached until a value of ω/ω_α is reached where after many cycles of computation a steady condition does not appear to exist. The flow changes from attached to separated and back to attached and back and forth without any definite pattern. Further increase in ω/ω_α will result in a steady condition with separated flow over the airfoil. A maximum in the amplitude of oscillation of the airfoil is reached in the vicinity of $\omega/\omega_\alpha = 1$ and the amplitude and phase curves behave like those for a linear oscillator. However, upon increasing ω/ω_α, breaks in the curves are again detected and for the two smaller values of Q_0, i.e. $Q_0 = 0.25$ and 0.5×10^{-3}, there is a small region of unsteadiness where the flow does not settle either to the attached or separated conditions, but beyond which the curves reach a steady condition again with the airfoil oscillating in the unstalled state. For the larger values of Q_0, no steady conditions can be reached. The failure to reach steady oscillations when the flow changes from attached to separated or vice versa in those regions where the breaks occur is probably due to the method of calculating C_N and C_M from Equations (7) and (13). At each step in the numerical finite difference scheme, the local values of α and $\dot{\alpha}$ are used to compute the local pitch rate A and α_W. These are then substituted into Equation (4) to evaluate a value of α_{Dm}. Depending on whether α is greater or less than α_{Dm}, the flow is taken to be either separated or attached accordingly. In the first transition region, the amplitude α is initially smaller than α_{Dm} and the flow is attached. As the amplitude grows, α will exceed α_{Dm} and the flow separates. Because of the ensuing increase in damping α then decreases and the flow becomes attached again with a smaller value of damping. The value of α then starts to increase and the cycle repeats itself. The same phenomenon also occurs in the second transition region. To eliminate this oscillation between attached and separated flows, a different scheme to fix the state of the flow at transition has to be devised.

Instead of holding k constant, Figures 10 and 11 show the amplitude and phase by varying the frequency of the external moment for the airfoil at $\alpha_m = 7.48°$, $Q_0 = 0.5 \times 10^{-3}$ and natural frequencies of 24, 48, 64 and 80 Hz. These curves show the same characteristics as those in Figures 8

and 9. The regions of unsteadiness where the flow changes from either attached to separated flows or vice versa are much larger for low natural frequencies.

The results given so far are for $\zeta_\alpha = 0$. For small values of the damping ratio ζ_α, Figure 12 shows a typical modification of the response curve at $k = 0.165$ and $Q_0 = 0.8 \times 10^{-3}$. Viscous damping tends to decrease the amplitude and increase slightly the region of unsteadiness where the flow oscillates between attached and separated states.

3.3 Forced Oscillations for Pitching and Plunging Motions

The empirical relations given in Section 2.1 for the unsteady aerodynamic loads are for pitching motion only. When the airfoil is oscillating in two-degree-of-freedom with large amplitudes of motion, a suitable method of representing the nonlinear aerodynamics has to be formulated. Experimental oscillatory data for the synethesization method have to include cases for various combinations of pitching and plunging amplitudes. These data are difficult to obtain and are not presently available.

The present investigation considers the case of a two-degree-of-freedom motion with large amplitude in pitch but small amplitude in plunge. In other words, the stiffness of the spring for plunging motion is kept large so that $\bar{\omega}$ in Equations (14) and (15) is large. The aerodynamic loads are then given by the sum of two terms: pitching motion from Equations (7) and (13) and plunging motion from linear aerodynamics given in Reference 1 using the indicial lift and moment functions at $M = 0.6$ determined by Mazelsky and Drischler (Ref. 17). This formulation of the aerodynamic loads is only approximate but it is used in this study to give some idea of the effect of a plunge degree of freedom motion with small amplitude on the pitching motion of the airfoil driven by an externally applied moment.

For an unstalled airfoil with $\alpha_m = 0.2°$, $\zeta_\alpha = \zeta_\xi = 0$, Figure 13 shows the pitch and plunge motions and the aerodynamic coefficients when steady conditions are reached. The value of the torsional natural frequency is $f_\alpha = 64$ Hz, $\bar{\omega} = 2$, $Q_0 = 0.5 \times 10^{-3}$ and the results are given for $\omega/\omega_\alpha = 2.2$ for cycles 35 to 40. In all computations, $\alpha(0) = \dot{\alpha}(0) = \xi(0) = \dot{\xi}(0) = 0$. The effects of f_α and $\bar{\omega}$ on the amplitude response with variation in ω/ω_α are shown in Figures 14 to 19. The amplitude of the pitching motion increases with decreasing $\bar{\omega}$ for the three values of f_α considered, that is, for the same value of the applied moment ($Q_0 = 0.5 \times 10^{-3}$), the presence of a plunging motion increases the pitch amplitude slightly. The second peak in the vicinity of $\bar{\omega}$ is usually quite small. For the ξ response curves shown in Figures 15, 17 and 19, the second peak is comparable to and in some cases larger than the first. However, it is not strongly dependent on f_α and its magnitude changes only slightly with increasing f_α which is quite unlike the first peak where the amplitude drops very rapidly as the torsional natural frequency is increased.

When the airfoil's mean angle of attack is increased to $\alpha_m = 7.48°$, the response is similar to that for one-degree-of-freedom motion discussed in the previous section (see Fig. 10). The effect of a plunge degree-of-freedom on the amplitude of the pitching motion is shown in Figure 20 for $f_\alpha = 64$ Hz, $Q_0 = 0.5 \times 10^{-3}$ and $\bar{\omega} = 10$, 4 and 3 respectively. For small values of ω/ω_α the flow is attached and the transition from attached to separated flow occurs around $\omega/\omega_\alpha = 1$. $\bar{\omega}$ does not appear to have much effect on the range of the unsteady region where the airfoil oscillates between attached and separated flow conditions. Unlike Figures 14, 16 and 18 which show a slight increase in the amplitude of α as $\bar{\omega}$ decreases, Figure 20 indicates the opposite, that is, for a stalled airfoil, introducing a plunge degree-of-freedom will decrease the amplitude of the pitch motion for the same magnitude of the externally applied moment. As ω ω_α increases, the flow becomes attached again. For large values of $\bar{\omega}$ ($\bar{\omega} = 10$ in this particular case), a steady condition is reached after approximately twenty cycles of forced oscillation. However, decreasing ω results in failure to achieve a steady condition even over 50 cycles of computation. The flow remains attached but the amplitudes of the pitch and plunge motions are scattered as shown in curves 2 and 3 of Figure 20. There is no plausible explanation for this anomaly at present.

4.0 CONCLUSIONS

The empirical relations used to represent nonlinear aerodynamic force and moment coefficient of both stalled and unstalled airfoils give fairly good results compared with the original loop data from which they are derived. They are formulated for pitching motion only and modifications have to be made if they are to be used for plunging or combination of plunging and pitching motions. The synthesized results can be used to derive data for any initial angle of attack of the airfoil, pitch amplitude and frequency of oscillation, but in the present formulation are restricted to the same airfoil and Mach number from which the experimental oscillatory aerodynamic data are obtained.

In one-degree-of-freedom forced oscillation in pitch, steady conditions for unstalled flow can be reached after a few cycles of motion of the airfoil starting from rest initially. For a stalled airfoil, usually a few more cycles of computations are required to reach steady state. In those cases where the flow changes from attached to separated or vice versa the transition regions are very unsteady and the flow is unsettled between the stalled and unstalled conditions without reaching a steady state, irrespective of the number of computation cycles carried out. Neither does a decrease in the time step used in the numerical finite-difference scheme show any improvement. This is probably due to an inadequate method used to compute the dynamic stall angle at those critical forcing frequencies. The inclusion of a viscous damping term in the dynamic equation of motion does not introduce any drastic changes in the behaviour of the response aside from a decrease in amplitude and slight increase in the unsteady region where the flow oscillates between attached and separated states.

For two-degree-of-freedom motion, only small plunge amplitude is considered because of the approximations used in computing the aerodynamic loads. The presence of a plunging motion increases the pitch amplitude slightly for attached flow, while a decrease in the pitch amplitude is predicted for separated flow.

5.0 REFERENCES

1. Bisplinghoff, R.L.; Ashley, H.; Halfman, R.L. — *Aeroelasticity.* Addison-Wesley Publishing Company, Inc., Cambridge, Mass., 1955.

2. Fung, Y.C. — *An Introduction to the Theory of Aeroelasticity.* John Wiley and Sons, N.Y., 1955.

3. Ballhaus, W.F.; Goorjian, P.M. — *Computation of Unsteady Transonic Flows by the Indicial Method.* AIAA Journal, Vol. 16, No. 2, 1978, pp. 117-124.

4. Rizzetta, D.P. — *Time-Dependent Response of a Two-Dimensional Airfoil in Transonic Flow.* AIAA Journal, Vol. 17, No. 1, 1979, pp. 26-32.

5. Yang, T.Y.; Chen, C.H. — *Transonic Flutter and Response Analysis of Two Three-Degree-of-Freedom Airfoils.* J. Aircraft, Vol. 19, No. 10, 1982, pp. 872-884.

6. Bathe, K.J.; Wilson, E.L. — *Numerical Methods in Finite Element Analysis.* Prentice-Hall, Inc., Englewood Cliffs, New Jersey, 1976.

7. Houbolt, J.C. — *A Recurrence Matrix Solution for the Dynamic Response of Elastic Aircraft.* Journal Aeronautical Sciences, Vol. 17, 1950, pp. 540-550.

8. Jones, D.J.
   Lee, B.H.K.
   Time Marching Numerical Solution of the Dynamic Response of Nonlinear Systems.
   National Research Council Canada, NAE-AN-25, January 1985.

9. Carta, F.O.
   Casellini, L.M.
   Arcidiacono, P.J.
   Elman, H.L.
   Analytical Study of Helicopter Rotor Stall Flutter.
   Reprint No. 413, Proceedings of the 26th Annual National Forum of the American Helicopter Society, Washington, D.C., June 1970.

10. Liiva, Jaan
    Unsteady Aerodynamic and Stall Effects on Helicopter Rotor Blade Airfoil Sections.
    J. of Aircraft, Vol. 6, No. 1, 1969, pp. 46-51.

11. Bielawa, R.L.
    Synthesized Unsteady Airfoil Data with Applications to Stall Flutter Calculations.
    Proceedings of the 31st Annual National Forum of the American Helicopter Society, Washington, D.C., May 1975.

12. Tran, C.T.
    Petot, D.
    Semi-Empirical Model for the Dynamic Stall of Airfoils in View of the Application to the Calculation of the Responses of a Helicopter Blade in Forward Flight.
    Paper No. 48, Sixth European Rotorcraft and Powered Lift Aircraft Forum, Bristol, England, Sept. 16-19, 1980.

13. Beddoes, T.S.
    A Synthesis of the Unsteady Aerodynamic Effect Including Stall Hysteresis.
    Vertica, Vol. 1, 1976, pp. 113-123.

14. Bielawa, R.L.
    Johnson, S.A.
    Chi, R.M.
    Gangawani, S.T.
    Aeroelastic Analysis for Propellers.
    NASA Contractor Rept. 3719, Dec. 1983.

15. Gray, L.
    Liiva, Jaan
    Two-Dimensional Tests of Airfoil Oscillating Near Stall.
    Vol. II, Data Report, USAAVLABS Tech. Rept. 68-13B, USAAMRDL, Ft. Eustis, VA., April, 1968.

16. Powell, M.J.D.
    A Method of Minimizing a Sum of Squares of Non-Linear Functions Without Calculating Derivatives.
    Computer Journal, Vol. 7, No. 4, 1965, pp. 303-307.

17. Mazelsky, B.
    Drischler, J.A.
    Numerical Determination of Indicial Lift and Moment Functions for a Two-Dimensional Sinking and Pitching Airfoil at Mach Numbers 0.5 and 0.6.
    NACA TN 2739, July, 1952.

TABLE 1

COEFFICIENTS IN EMPIRICAL RELATIONS FOR SYNTHESIZED DATA

The coefficients for the synthesized data given in Equations (4) to (13) are as follows:

ϵ = -0.09887 C_{Am} = 0.43095 C_{Wm} = 0.40729

C_{AR} = 0.66471 C_{WR} = -0.08279 C_{At} = 0.07816

$C_{\alpha t}$ = 0.00959

P	1	2	3	4	5
	0.27904	0.24569	-0.12087	-0.13962	0.01926

P	6	7	8	9	10
	0.22186	0.09565	0.00059	-0.06892	-0.00099

Q	1	2	3	4	5	6	7
	-0.03123	-0.00345	0.00026	-0.00215	0.09170	-0.01914	0.00003

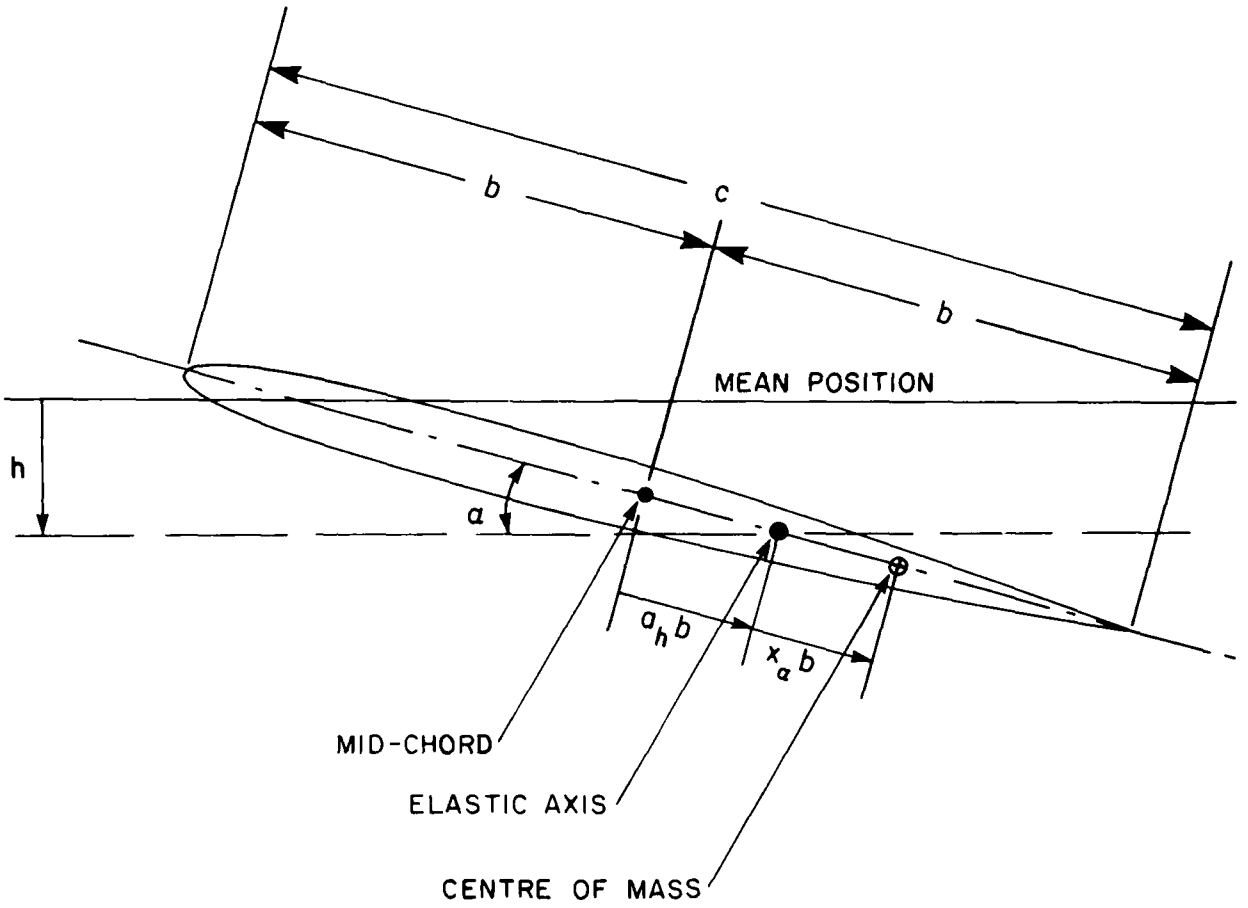

FIG. 1: TWO-DEGREE-OF-FREEDOM AIRFOIL MOTION

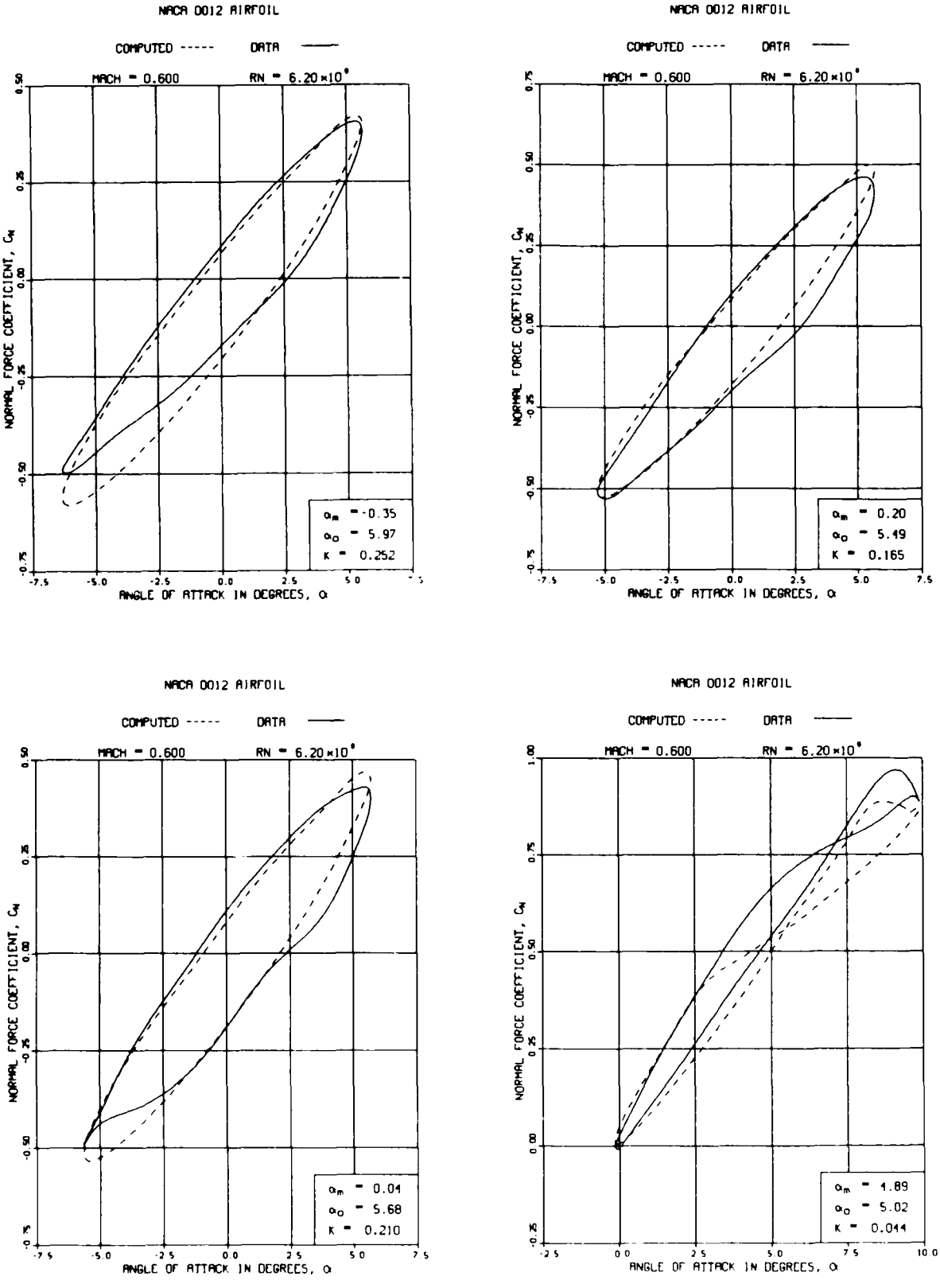

FIG. 2: COMPARISON OF SYNTHESIZED NORMAL FORCE COEFFICIENT LOOPS WITH TEST DATA FOR VERTOL MODIFIED NACA0012 AIRFOIL, M = 0.6, $R_e = 6.2 \times 10^6$ (Cont'd)

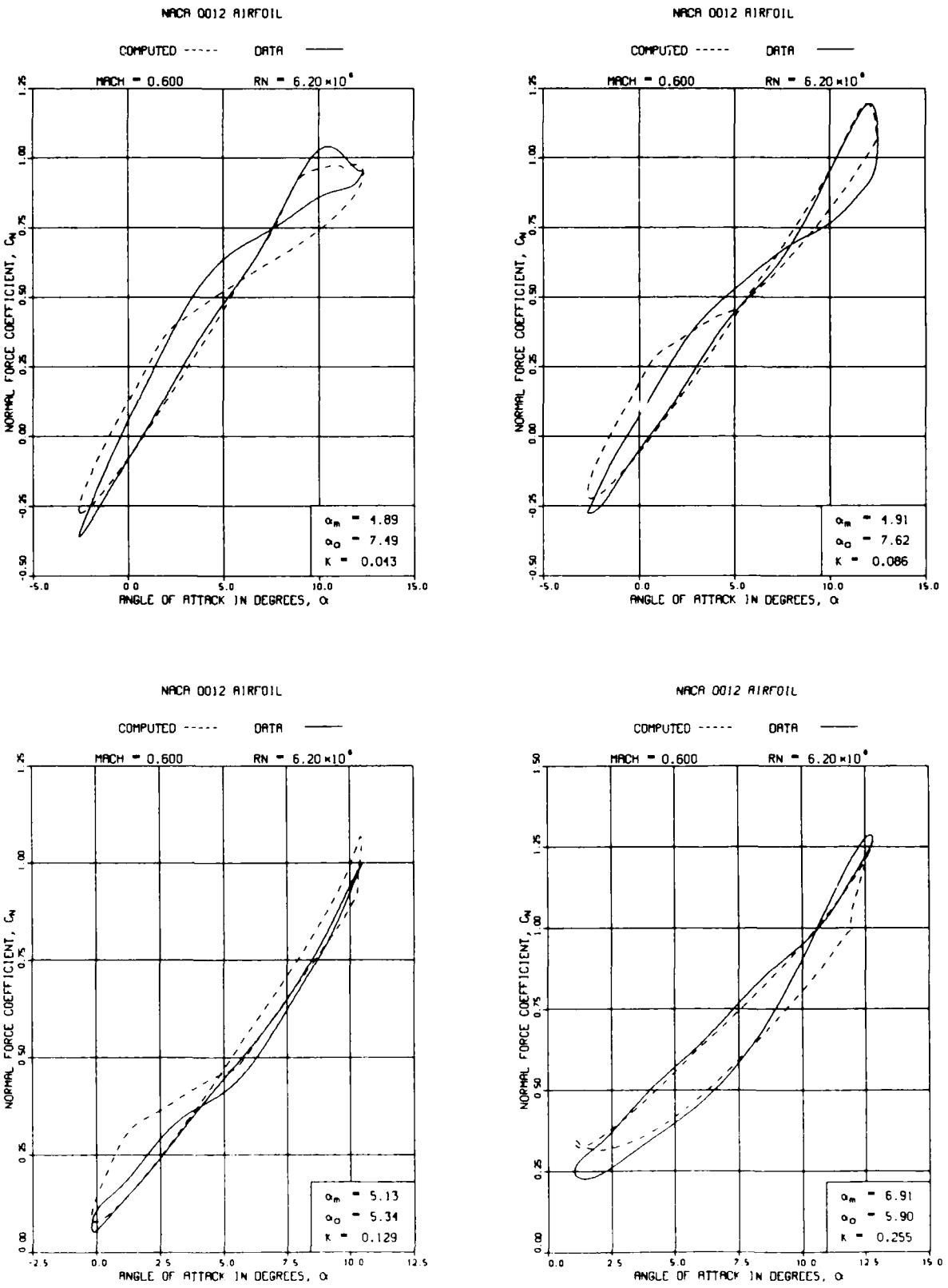

FIG. 2: COMPARISON OF SYNTHESIZED NORMAL FORCE COEFFICIENT LOOPS WITH TEST DATA FOR VERTOL MODIFIED NACA0012 AIRFOIL, M = 0.6, $R_e = 6.2 \times 10^6$ (Cont'd)

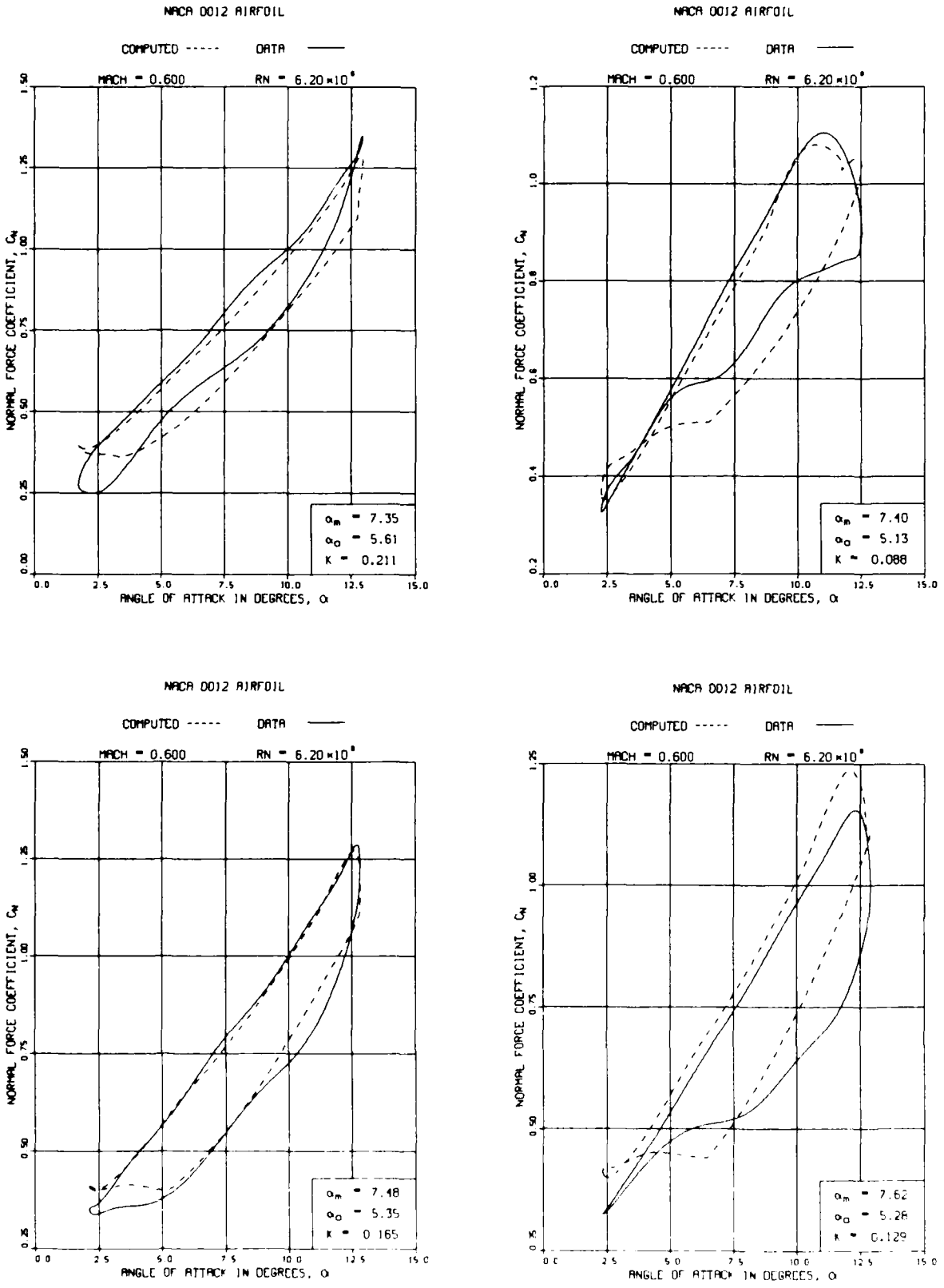

FIG. 2: COMPARISON OF SYNTHESIZED NORMAL FORCE COEFFICIENT LOOPS WITH TEST DATA FOR VERTOL MODIFIED NACA0012 AIRFOIL, M = 0.6, $R_e = 6.2 \times 10^6$ (Cont'd)

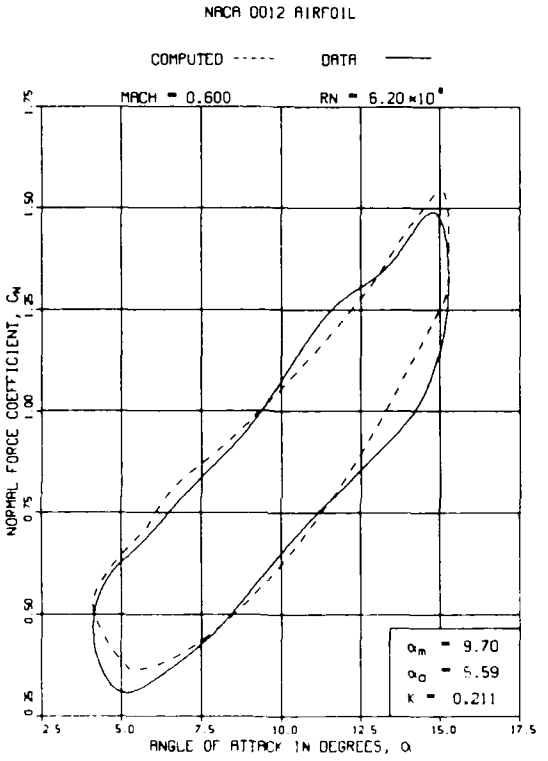

FIG. 2: COMPARISON OF SYNTHESIZED NORMAL FORCE COEFFICIENT LOOPS WITH TEST DATA FOR VERTOL MODIFIED NACA0012 AIRFOIL, M = 0.6, $R_e = 6.2 \times 10^6$

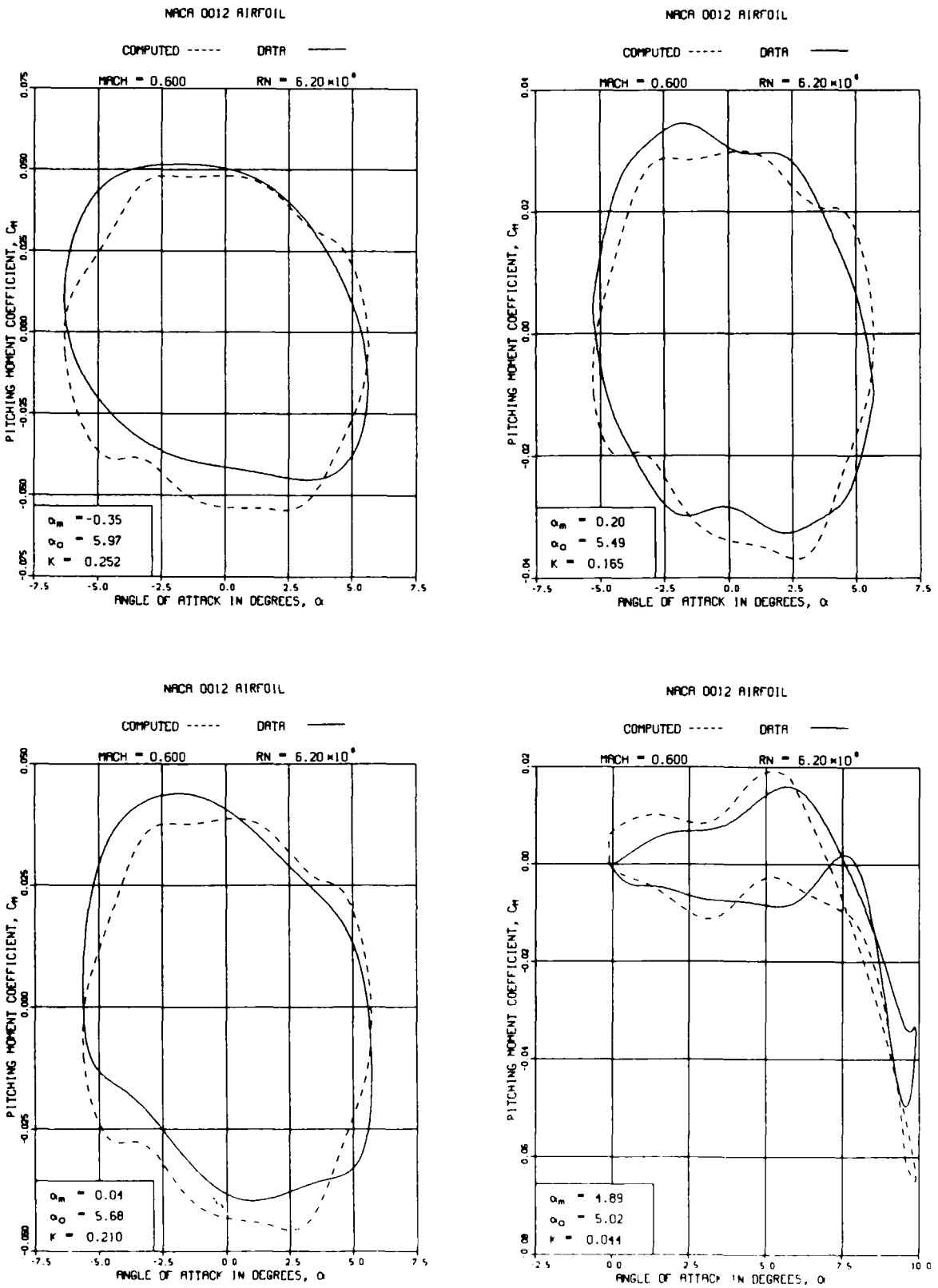

FIG. 3: COMPARISON OF SYNTHESIZED PITCHING MOMENT COEFFICIENT LOOPS WITH TEST DATA FOR VERTOL MODIFIED NACA0012 AIRFOIL, M = 0.6, R_e = 6.2 × 10^6 (Cont'd)

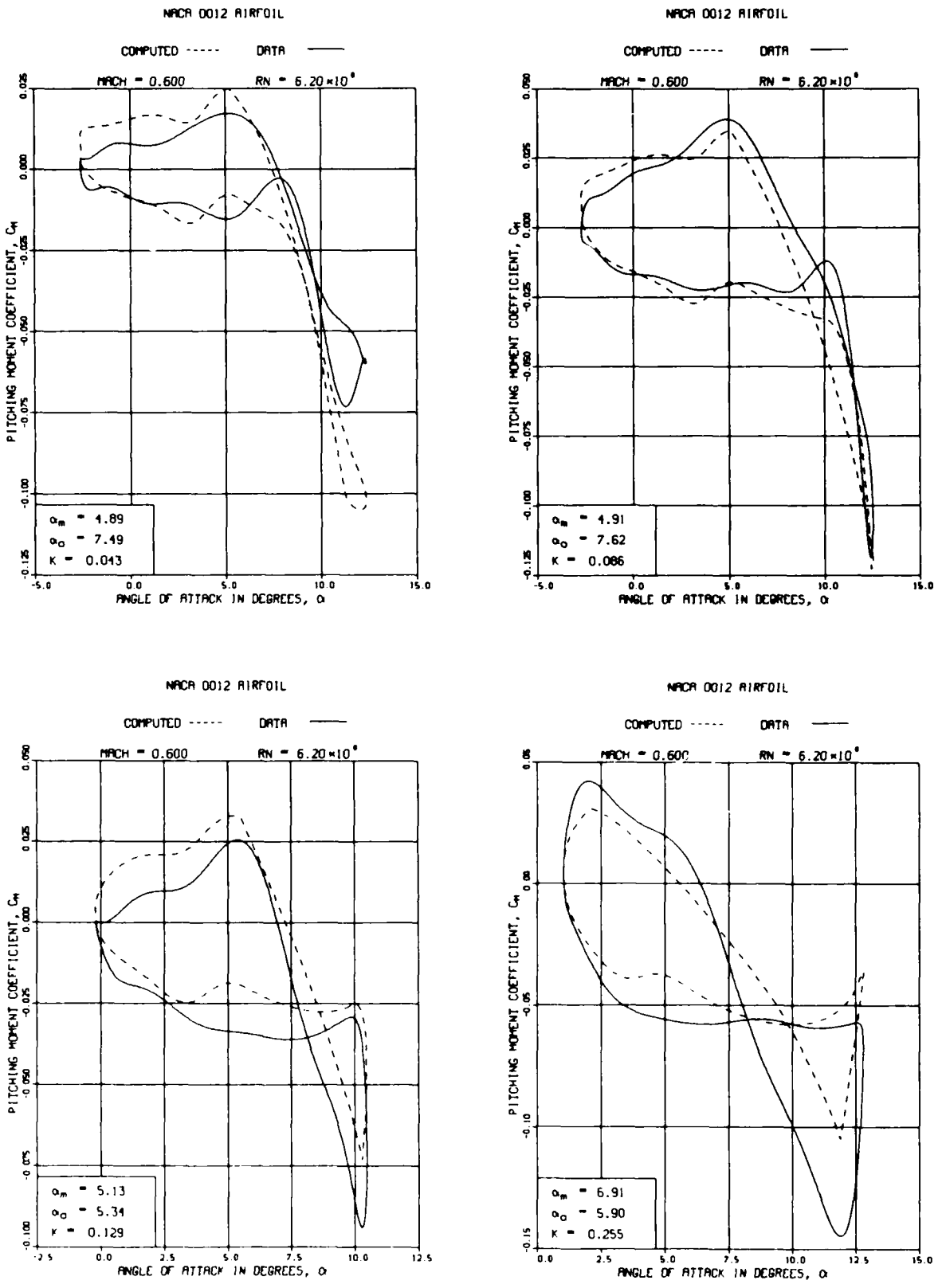

FIG. 3: COMPARISON OF SYNTHESIZED PITCHING MOMENT COEFFICIENT LOOPS WITH TEST DATA FOR VERTOL MODIFIED NACA0012 AIRFOIL, M = 0.6, $R_e = 6.2 \times 10^6$ (Cont'd)

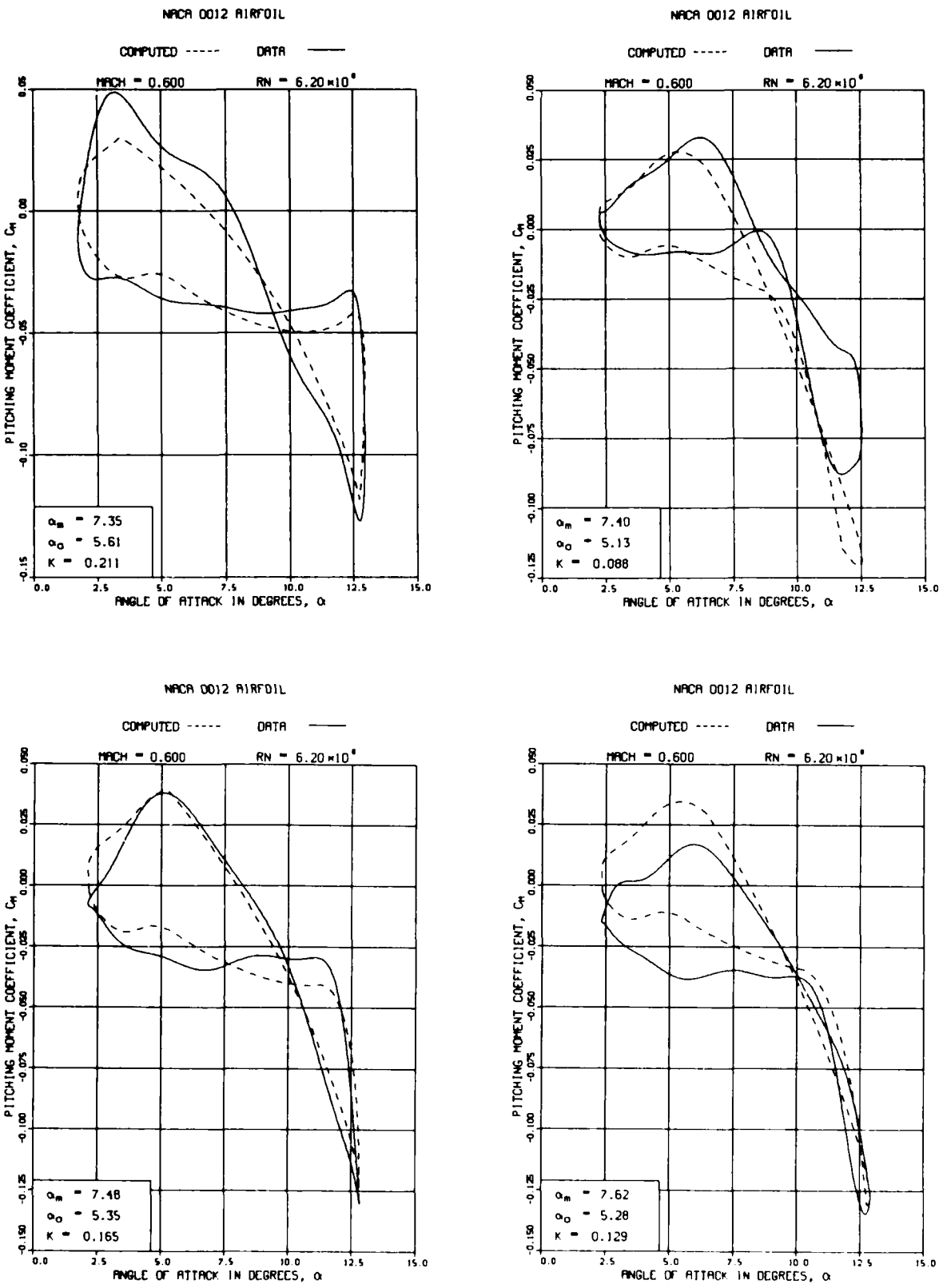

FIG. 3: COMPARISON OF SYNTHESIZED PITCHING MOMENT COEFFICIENT LOOPS WITH TEST DATA FOR VERTOL MODIFIED NACA0012 AIRFOIL, M = 0.6, R_e = 6.2 × 10^6 (Cont'd)

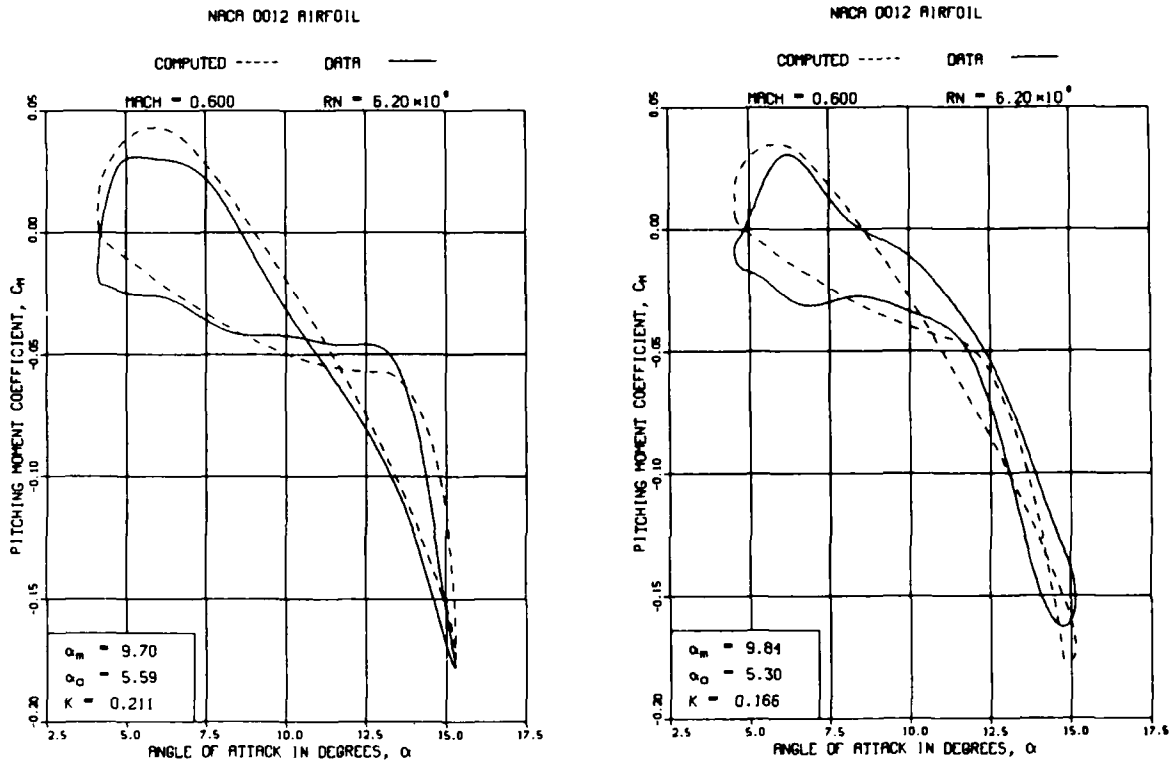

FIG. 3: COMPARISON OF SYNTHESIZED PITCHING MOMENT COEFFICIENT LOOPS WITH TEST DATA FOR VERTOL MODIFIED NACA0012 AIRFOIL, M = 0.6, R_e = 6.2 × 10^6

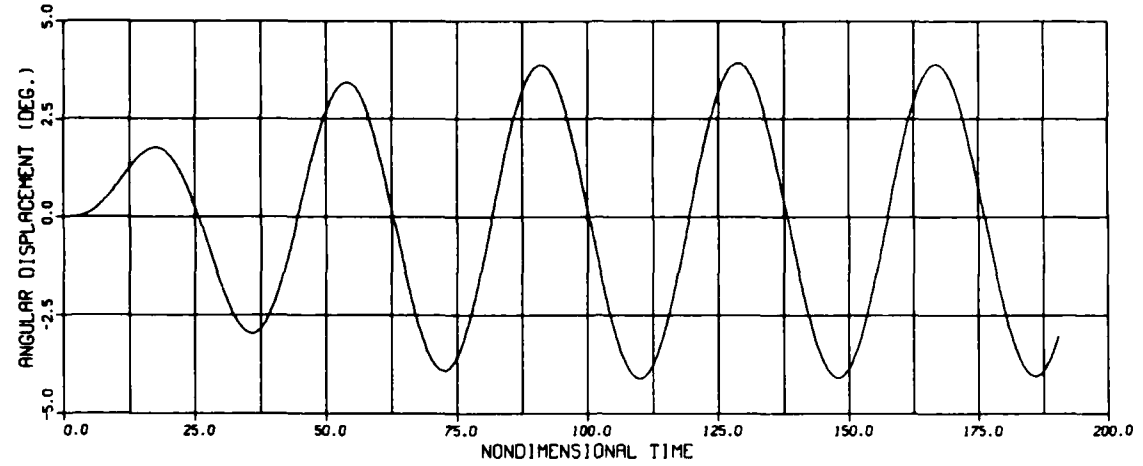

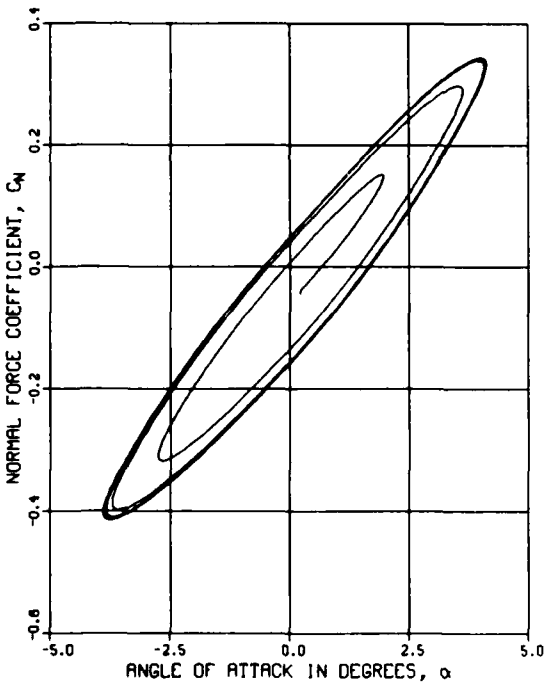

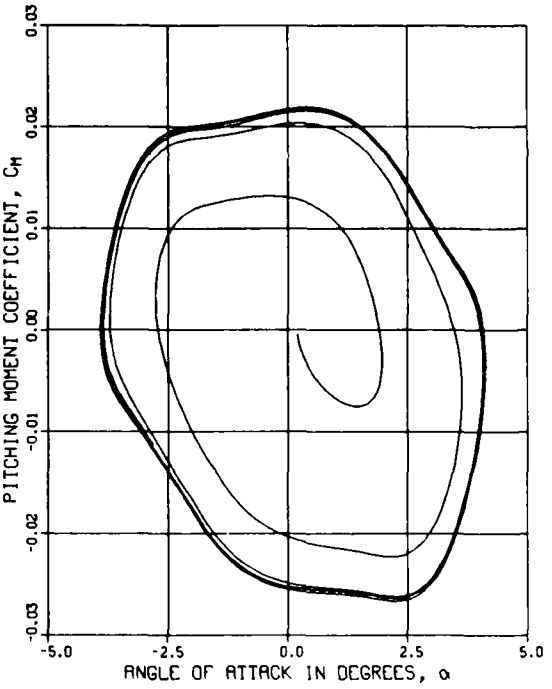

FIG. 4a: ANGULAR DISPLACEMENT FROM THE MEAN, C_N AND C_M FOR THE FIRST 5 CYCLES OF FORCED PITCH OSCILLATION, $\alpha_m = 0.2°$, $k = 0.165$, $Q_o = 0.8 \times 10^{-3}$ AND $\omega/\omega_\alpha = 0.9$

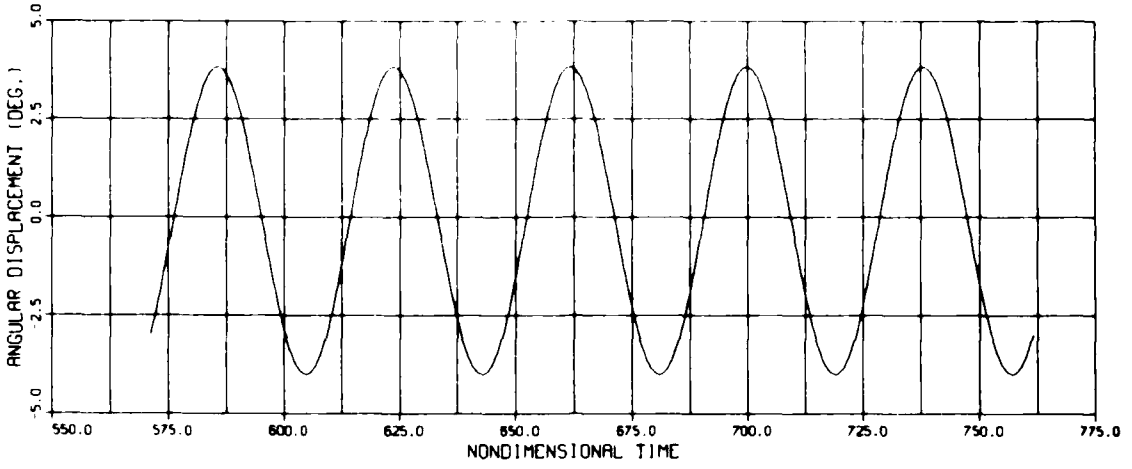

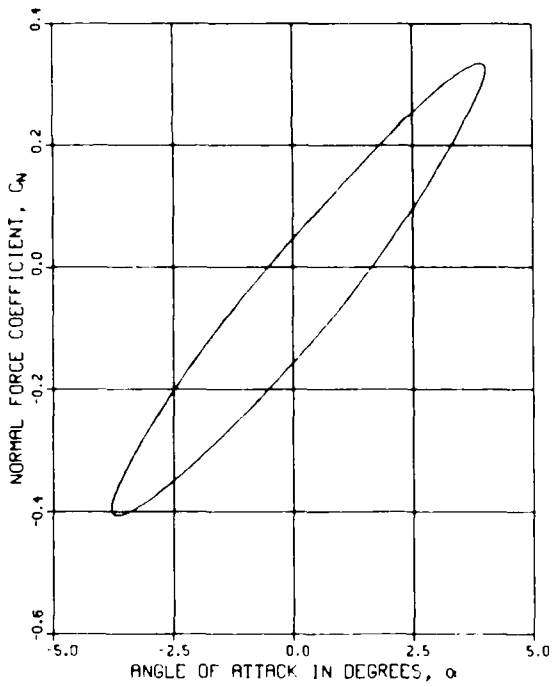

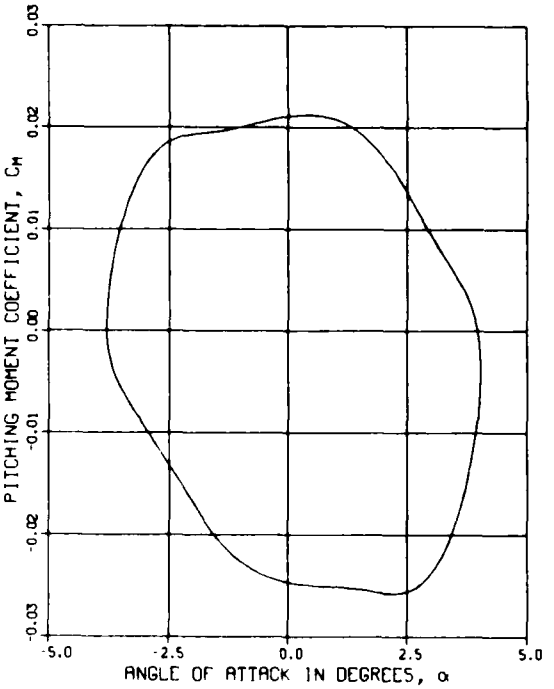

FIG. 4b: ANGULAR DISPLACEMENT FROM THE MEAN, C_N AND C_M FOR THE 15-20 CYCLES OF FORCED PITCH OSCILLATION, $\alpha_m = 0.2$, $k = 0.165$, $Q_o = 0.8 \times 10^{-3}$ AND $\omega/\omega_\alpha = 0.9$

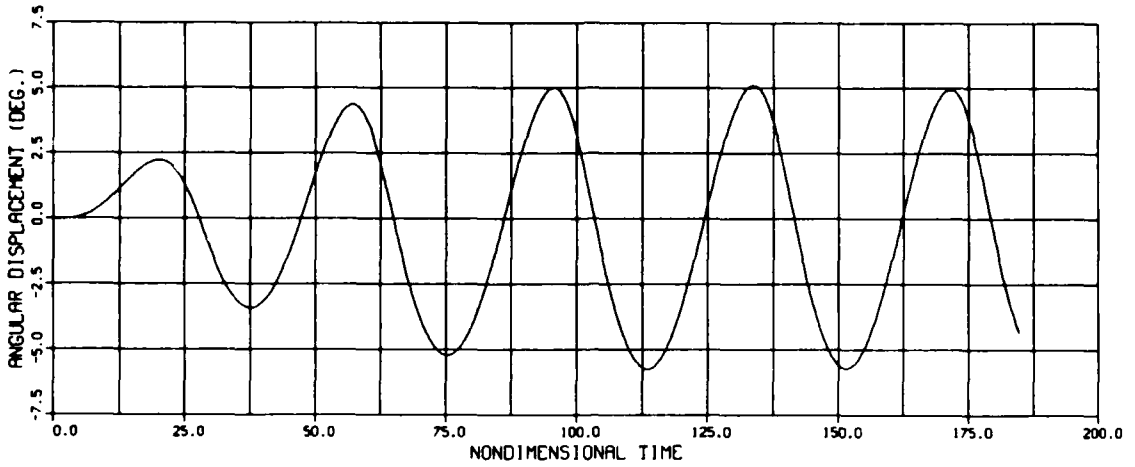

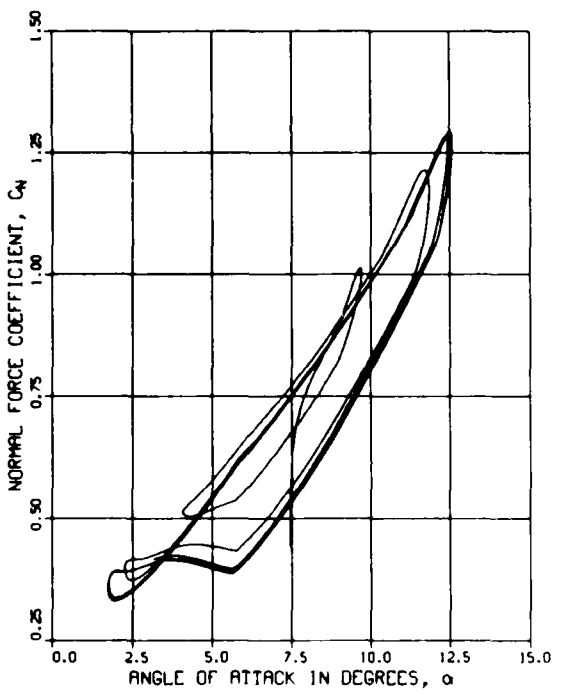

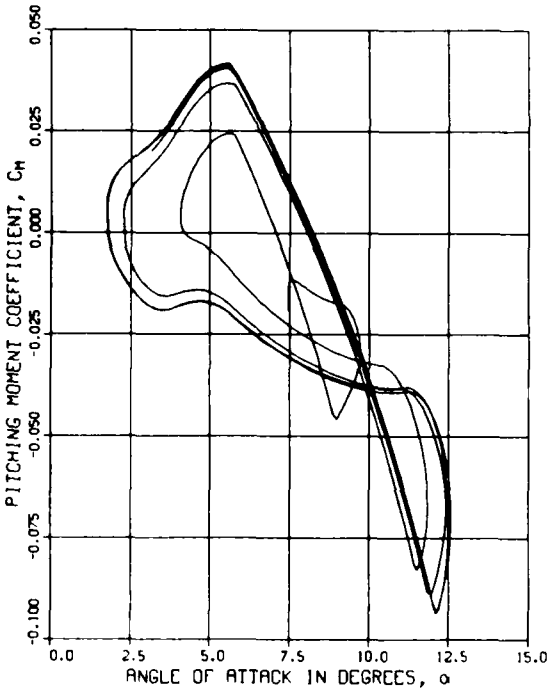

FIG. 5a: ANGULAR DISPLACEMENT FROM THE MEAN, C_N AND C_M FOR THE FIRST 5 CYCLES OF FORCED PITCH OSCILLATION, $\alpha_m = 7.48°$, $k = 0.165$, $Q_o = 0.5 \times 10^{-3}$ AND $\omega/\omega_\alpha = 1.4$

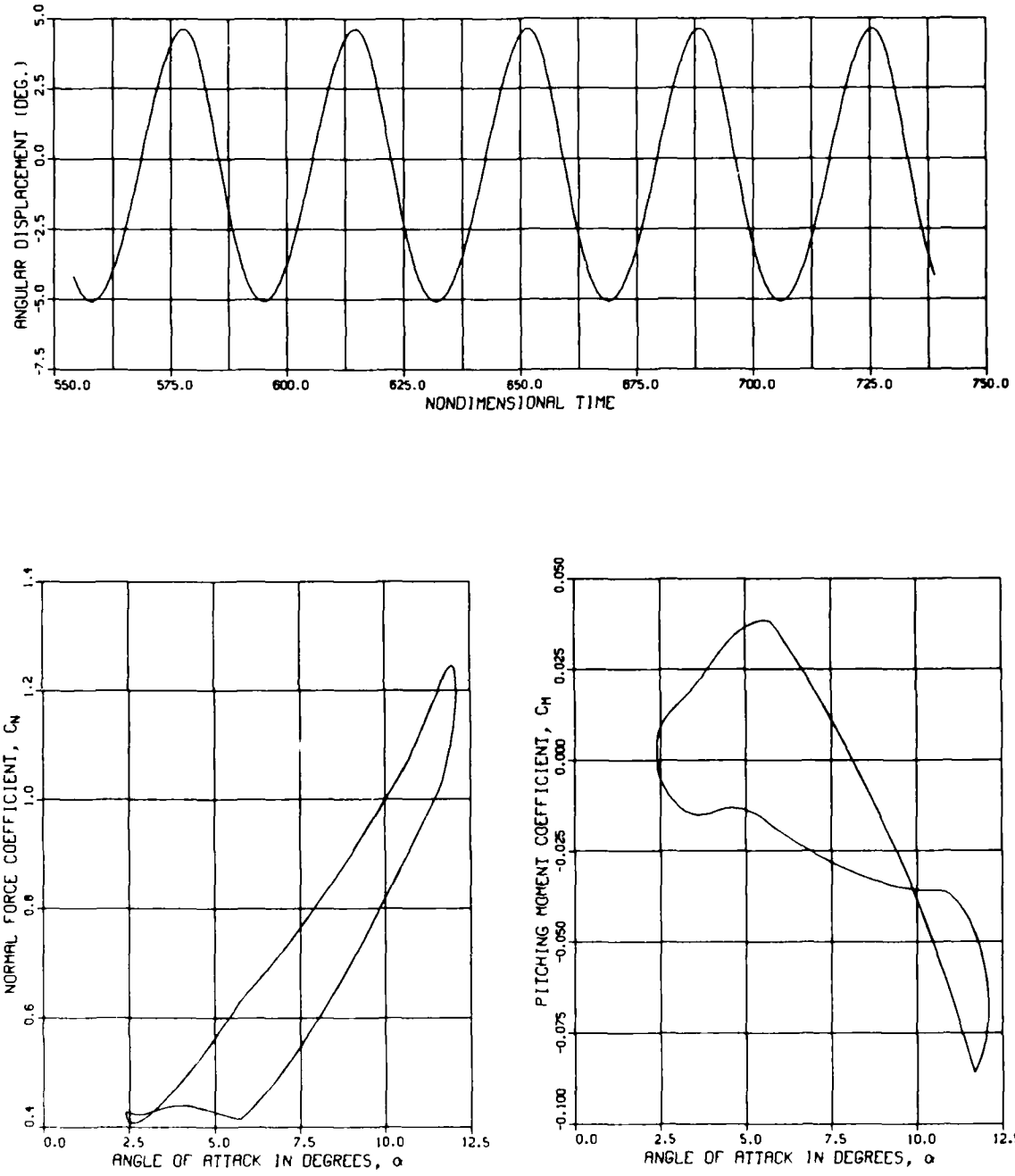

FIG. 5b: ANGULAR DISPLACEMENT FROM THE MEAN, C_N AND C_M FOR THE 15-20 CYCLES OF FORCED PITCH OSCILLATION, $\alpha_m = 7.48^\circ$, $k = 0.165$, $Q_o = 0.5 \times 10^{-3}$ AND $\omega/\omega_\alpha = 1.4$

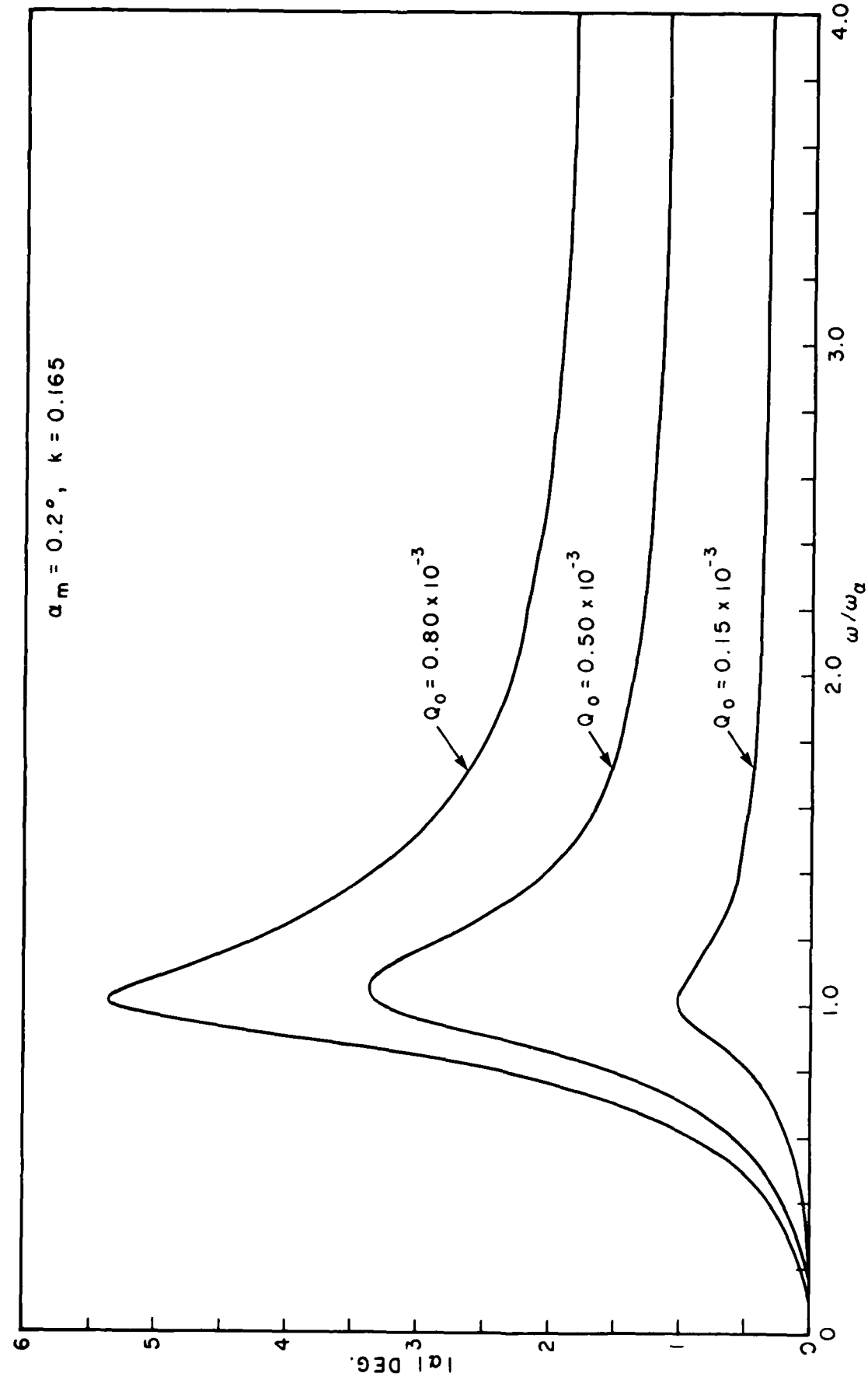

FIG. 6: VARIATION OF THE AMPLITUDE OF α WITH ω/ω_α FOR FORCED PITCH OSCILLATION, α_m = 0.2°, k = 0.165

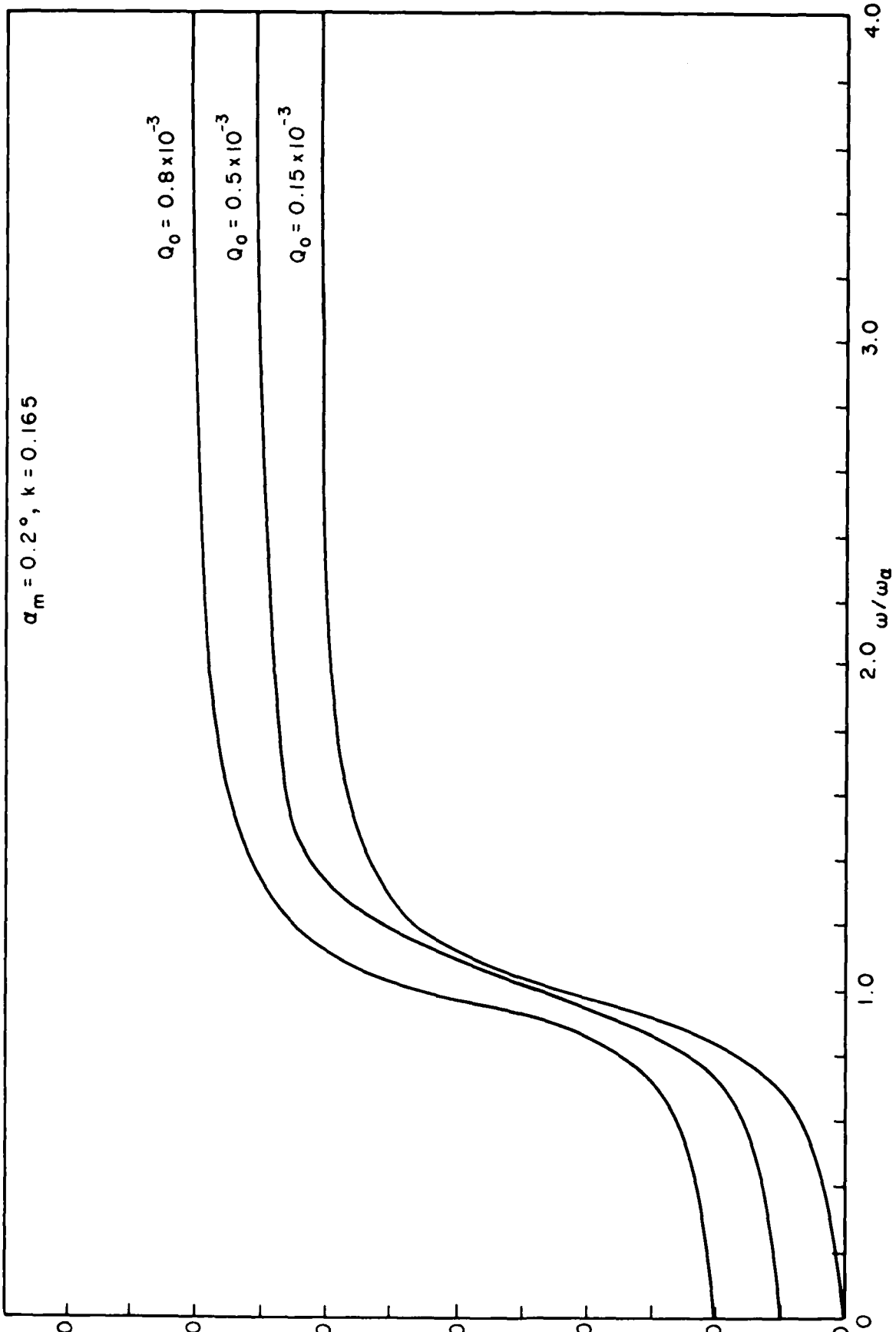

FIG. 7: VARIATION OF THE PHASE ANGLE OF α WITH ω/ω_α FOR FORCED PITCH OSCILLATION, $\alpha_m = 0.2°$, k = 0.165
(CURVES SHIFTED UPWARDS BY 20°)

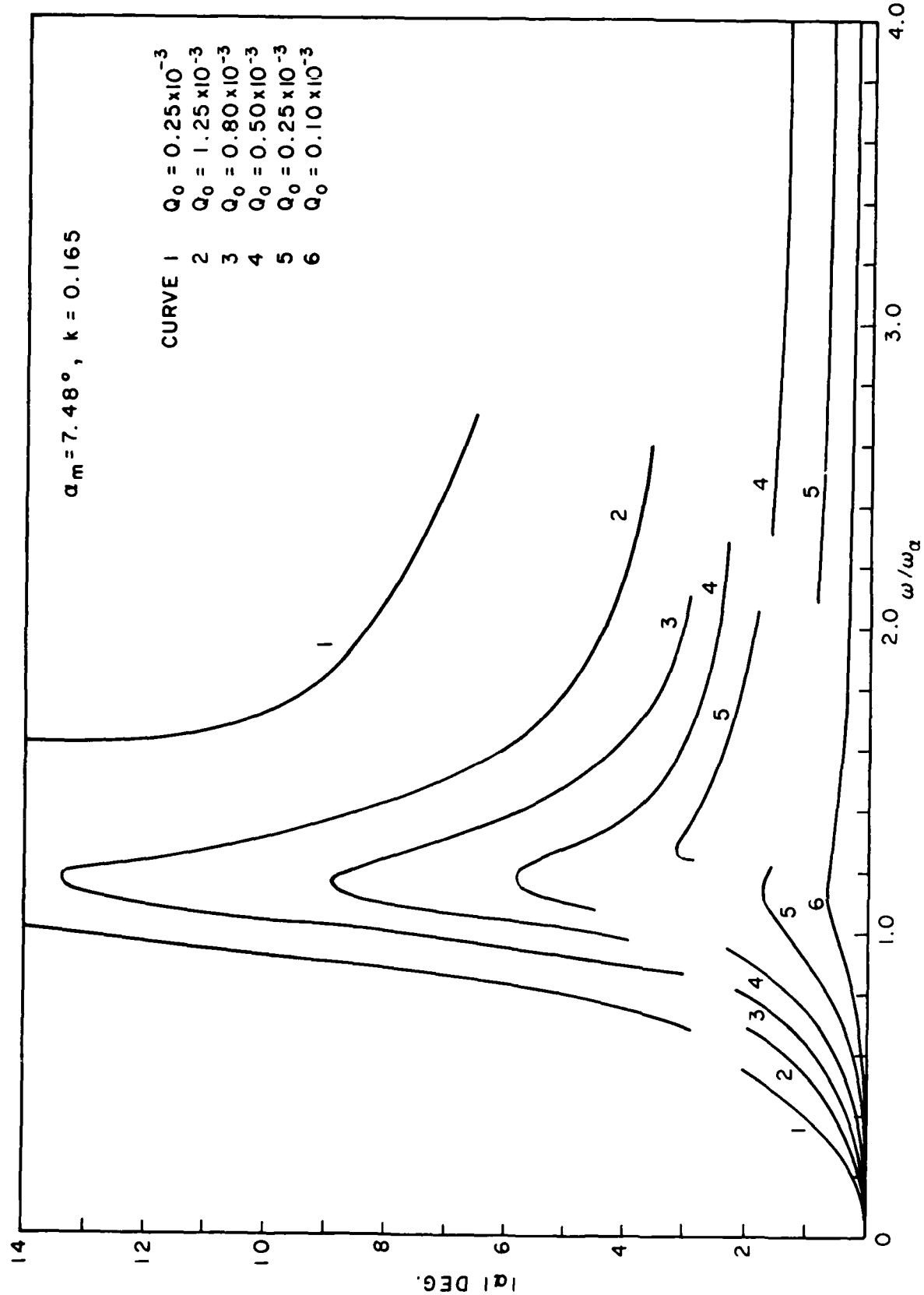

FIG. 8: VARIATION OF THE AMPLITUDE OF α WITH ω/ω_α FOR FORCED PITCH OSCILLATION, $\alpha_m = 7.48°$, k = 0.165

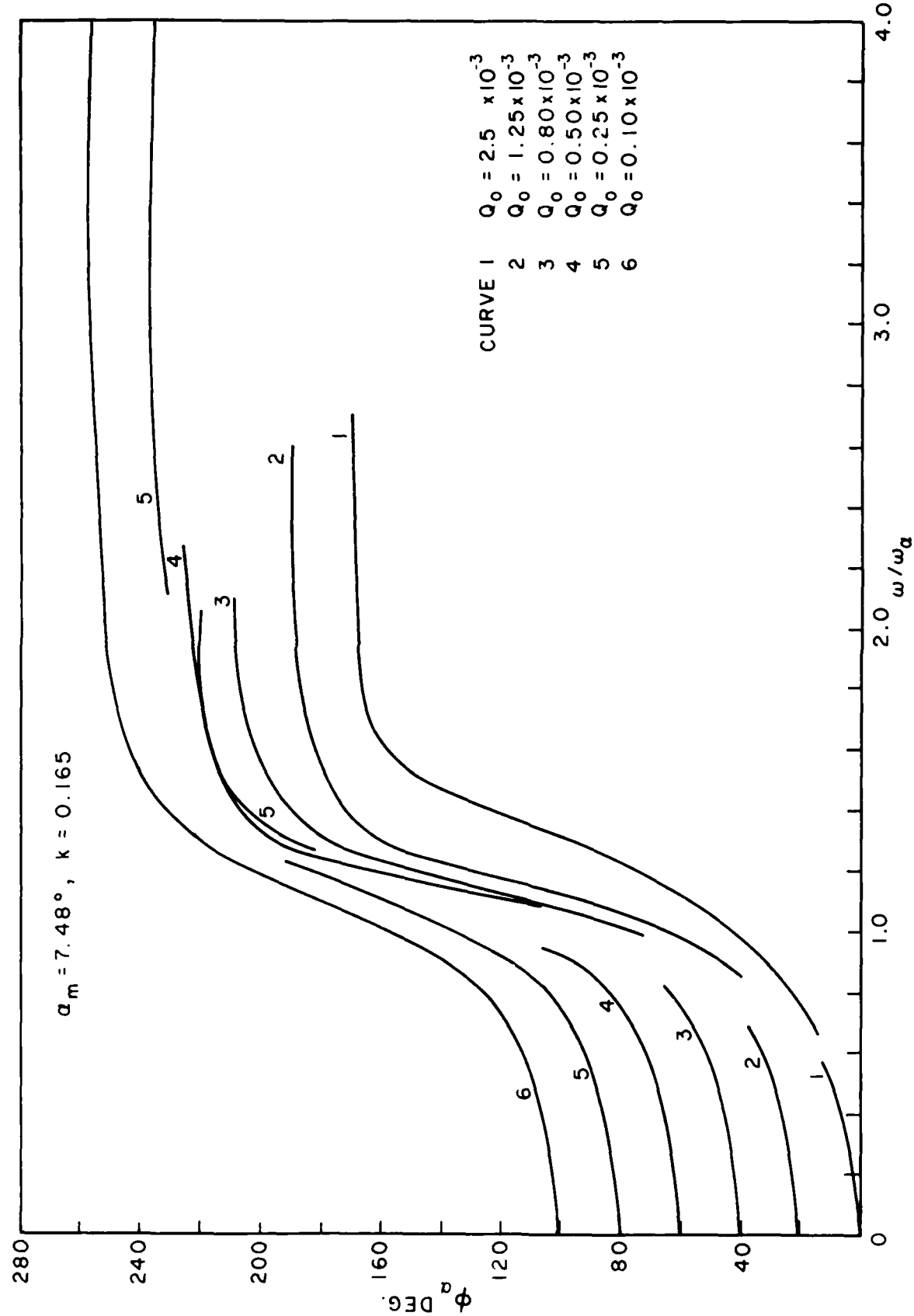

FIG. 9: VARIATION OF THE PHASE ANGLE OF α WITH ω/ω_α FOR FORCED PITCH OSCILLATION, $\alpha_m = 7.48°$, k = 0.165
(CURVES SHIFTED UPWARDS BY 20°)

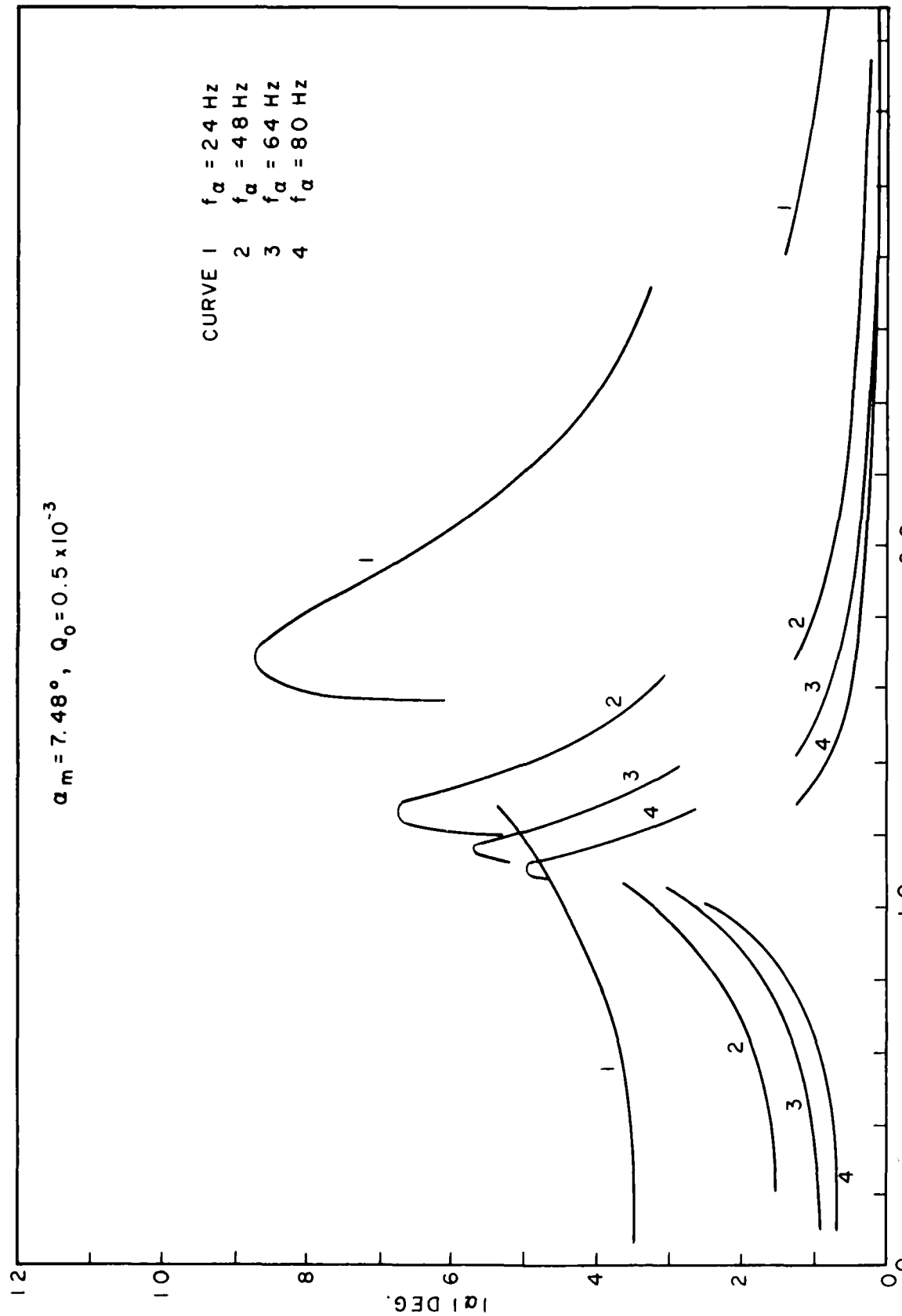

FIG. 10: VARIATION OF THE AMPLITUDE OF α WITH ω/ω_α FOR FORCED PITCH OSCILLATION, $\alpha_m = 7.48°$, $Q_0 = 0.5 \times 10^{-3}$

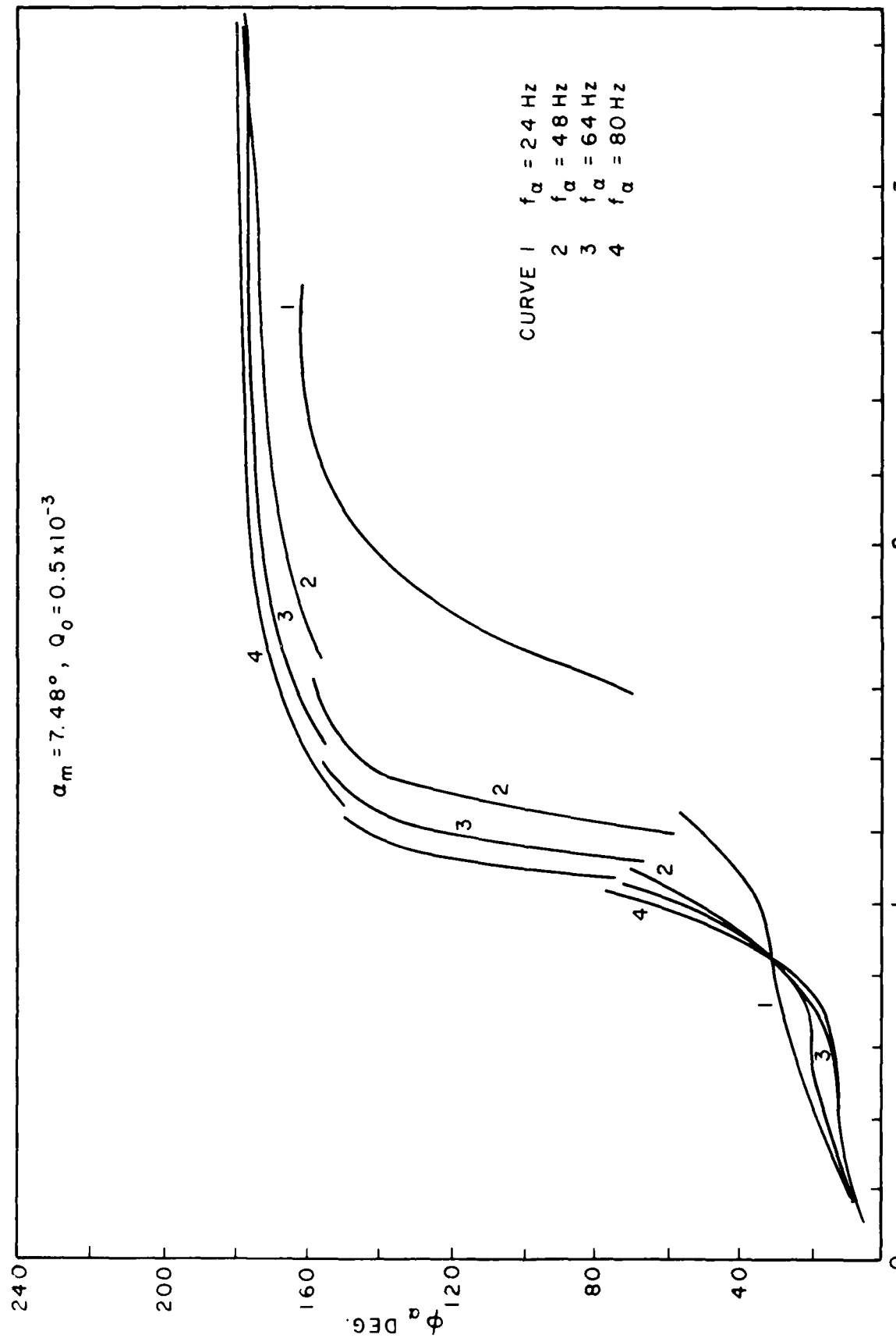

FIG. 11: VARIATION OF THE PHASE ANGLE OF α WITH ω/ω_α FOR FORCED PITCH OSCILLATION, $\alpha_m = 7.48°$, $Q_0 = 0.5 \times 10^{-3}$

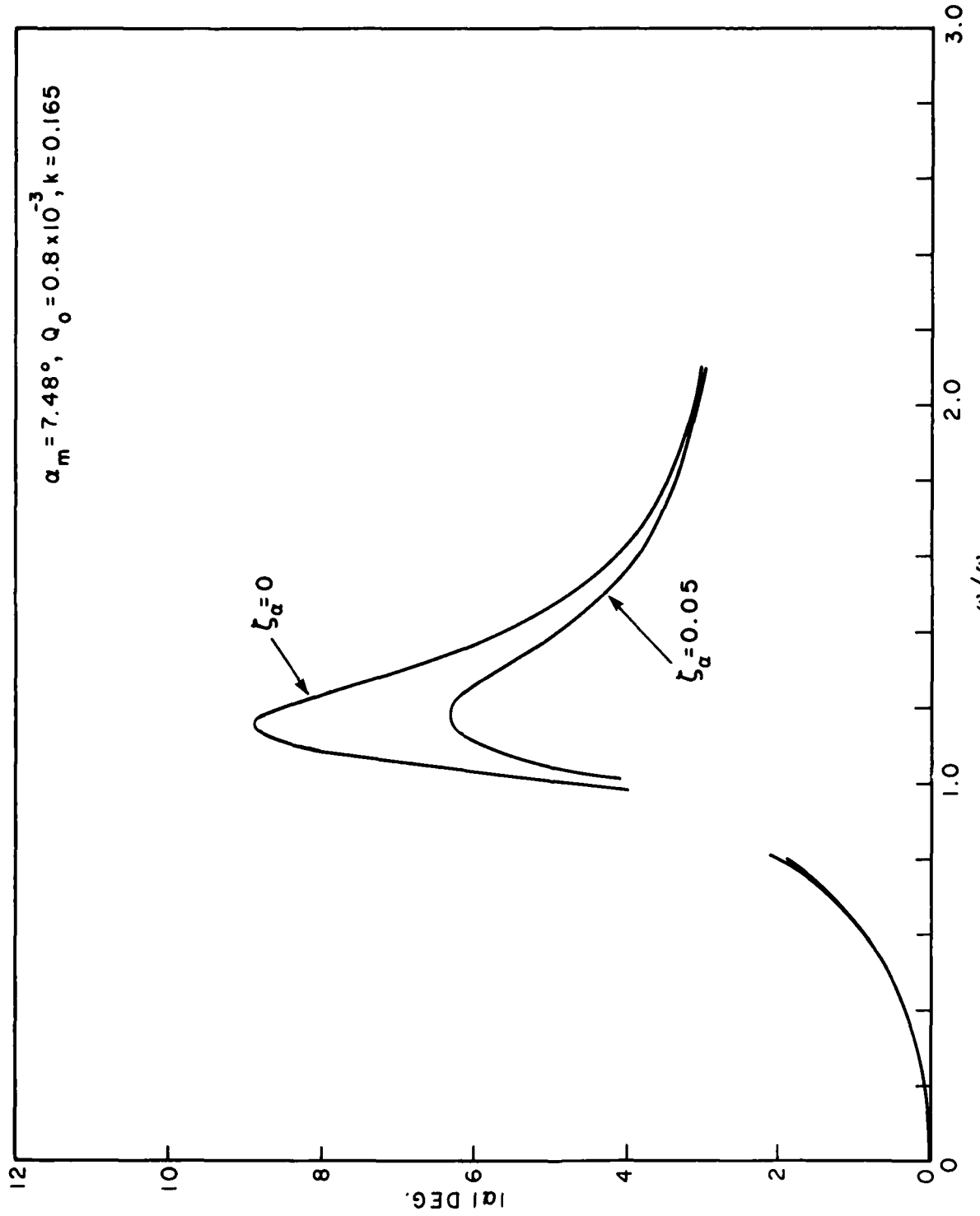

FIG. 12: EFFECT OF VISCOUS DAMPING ON THE AMPLITUDE RESPONSE OF α WITH ω/ω_α FOR FORCED PITCH OSCILLATION, $\alpha_m = 7.48°$, $Q_o = 0.8 \times 10^{-3}$

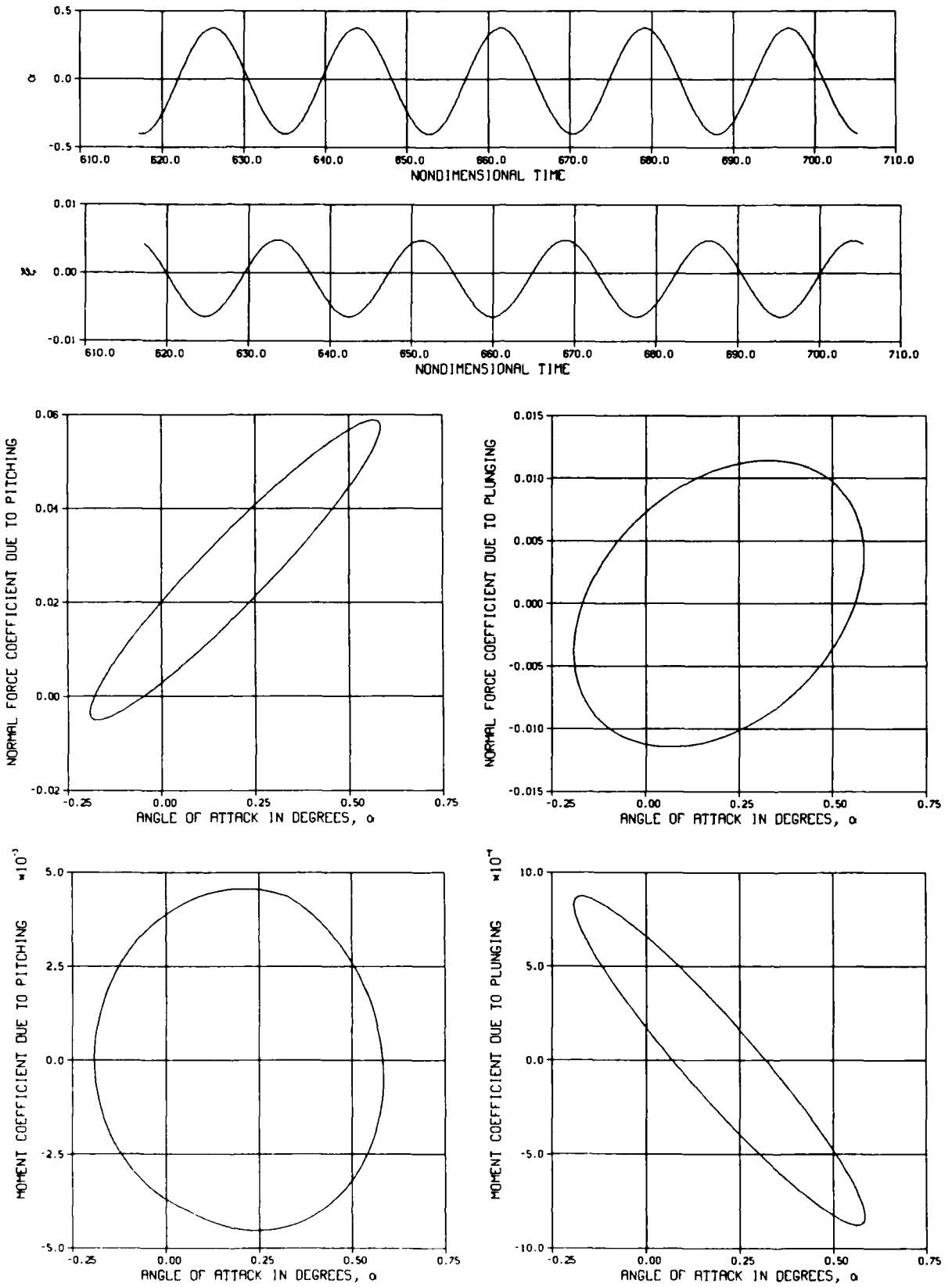

FIG. 13: α, ξ, C_N AND C_M FOR A TWO-DEGREE-OF-FREEDOM FORCED OSCILLATING AIRFOIL FOR THE 35-40 CYCLES, f_α = 64 Hz, $\bar{\omega}$ = 2, $Q_o = 0.5 \times 10^{-3}$ AND ω/ω_α = 2.2

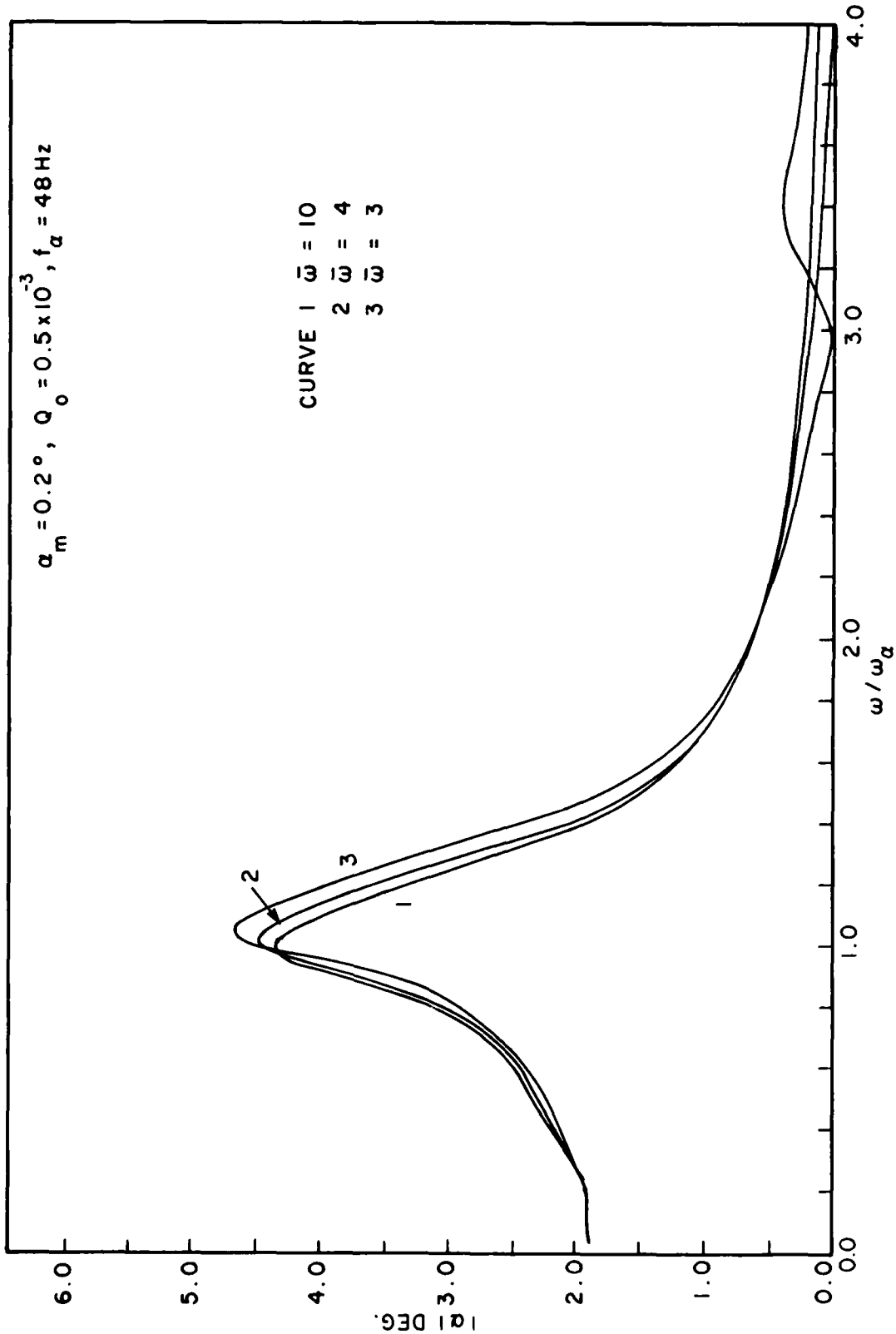

FIG. 14: VARIATION OF THE AMPLITUDE OF α WITH ω/ω_α FOR AN AIRFOIL OSCILLATING IN PITCH AND PLUNGE, $\alpha_m = 0.2°$, $f_\alpha = 48$ Hz AND $Q_o = 0.5 \times 10^{-3}$

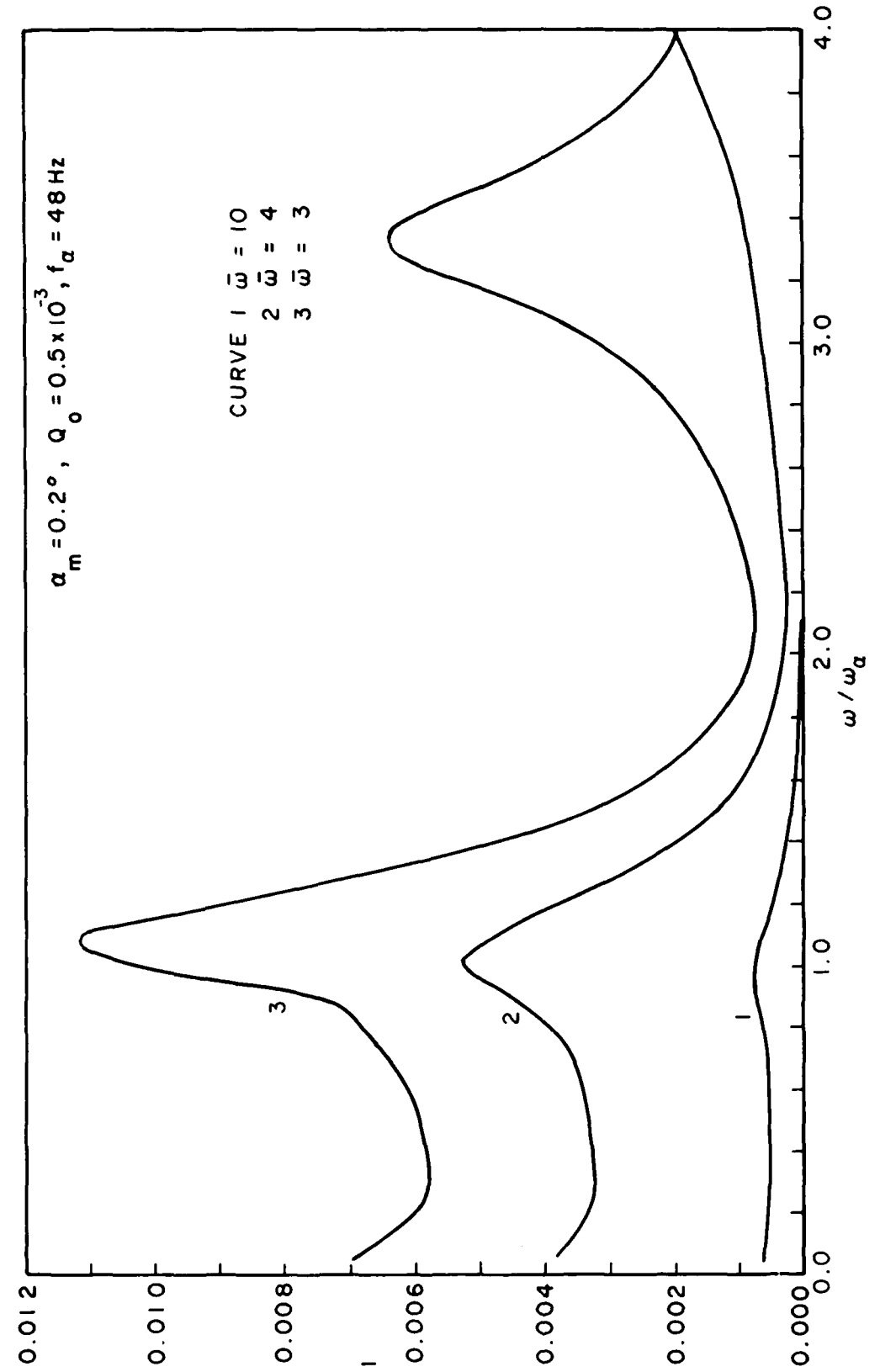

FIG. 15: VARIATION OF THE AMPLITUDE OF ξ WITH ω/ω_α FOR AN AIRFOIL OSCILLATING IN PITCH AND PLUNGE, $\alpha_m = 0.2°$, $f_\alpha = 48$ Hz AND $Q_o = 0.5 \times 10^{-3}$

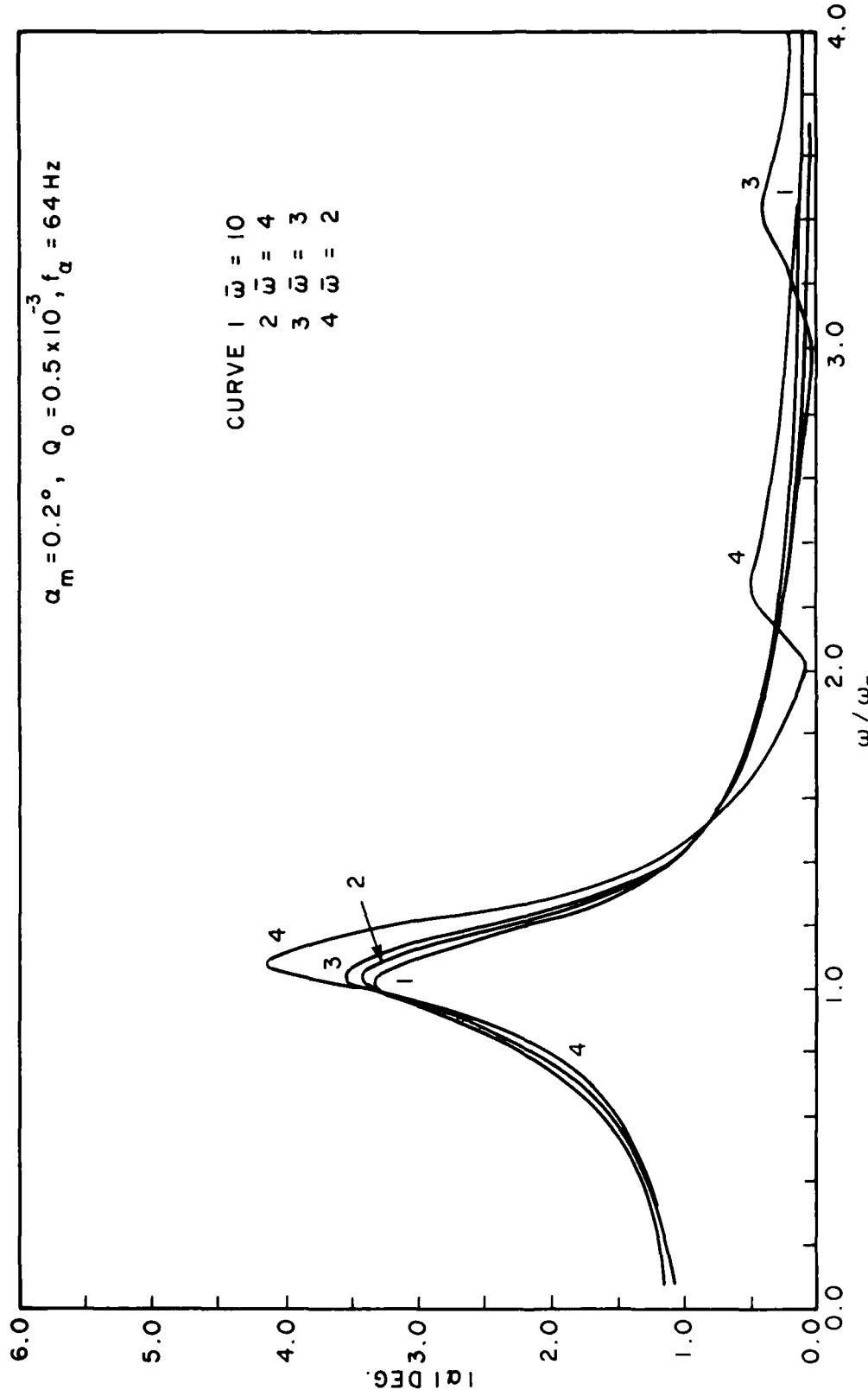

FIG. 16: VARIATION OF THE AMPLITUDE OF α WITH ω/ω_α FOR AN AIRFOIL OSCILLATING IN PITCH AND PLUNGE, α_m = 0.2°, f_α = 64 Hz AND Q_o = 0.5 × 10^{-3}

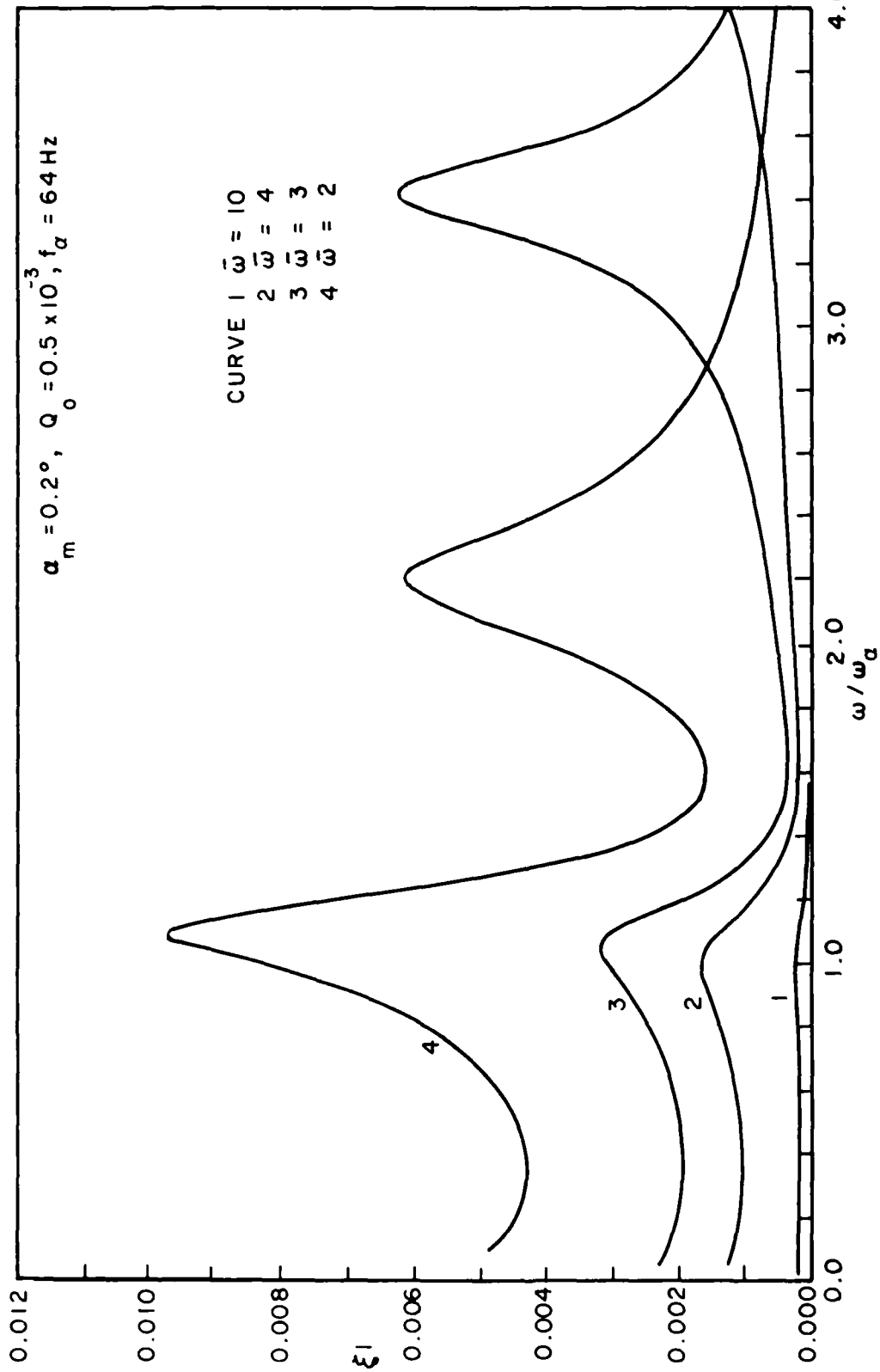

FIG. 17: VARIATION OF THE AMPLITUDE OF ξ WITH ω/ω_α FOR AN AIRFOIL OSCILLATING IN PITCH AND PLUNGE, α_m = 0.2°, f_α = 64 Hz AND Q_o = 0.5 × 10^{-3}

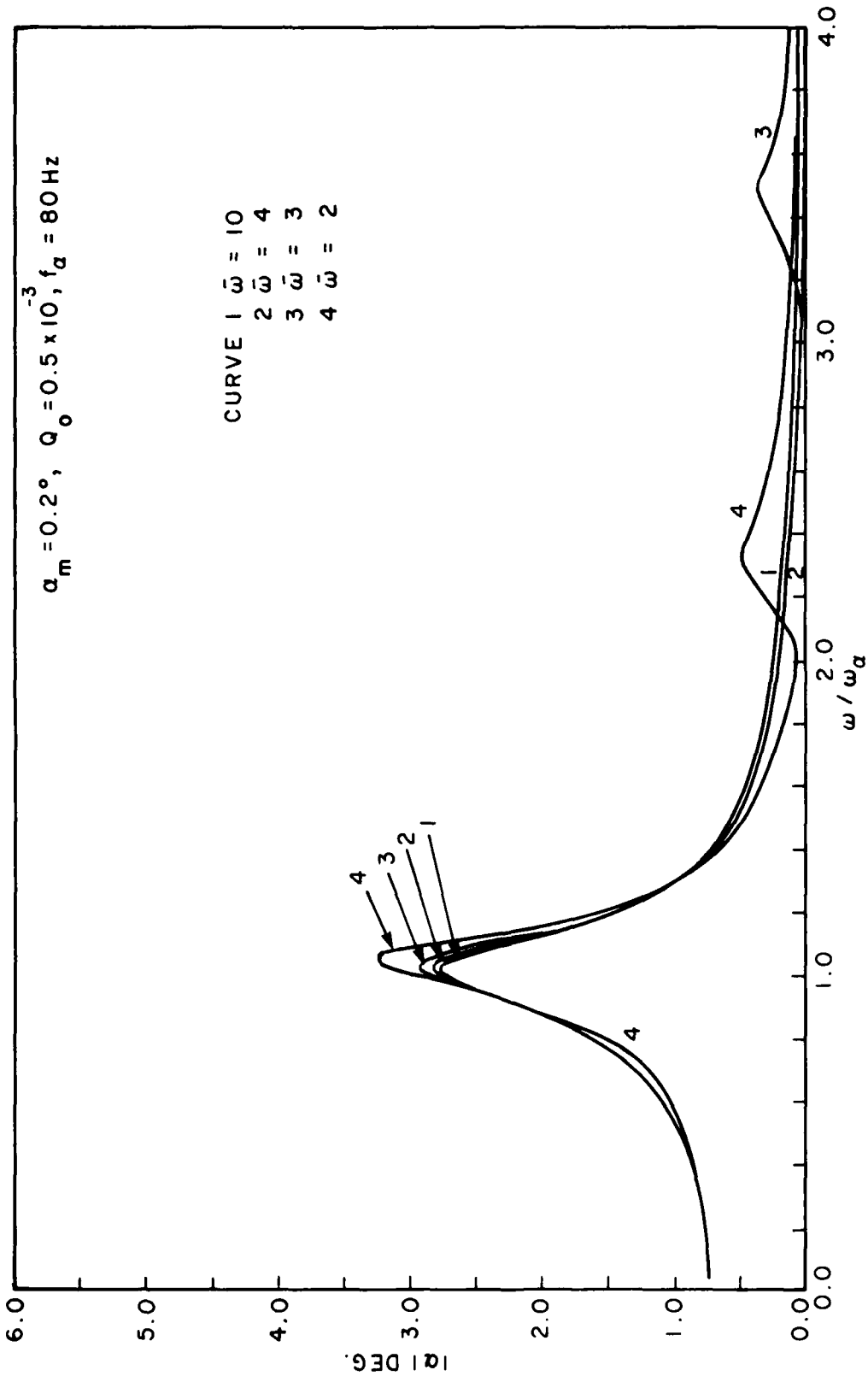

FIG. 18: VARIATION OF THE AMPLITUDE OF α WITH ω/ω_α FOR AN AIRFOIL OSCILLATING IN PITCH AND PLUNGE, $\alpha_m = 0.2°$, $f_\alpha = 80$ Hz AND $Q_o = 0.5 \times 10^{-3}$

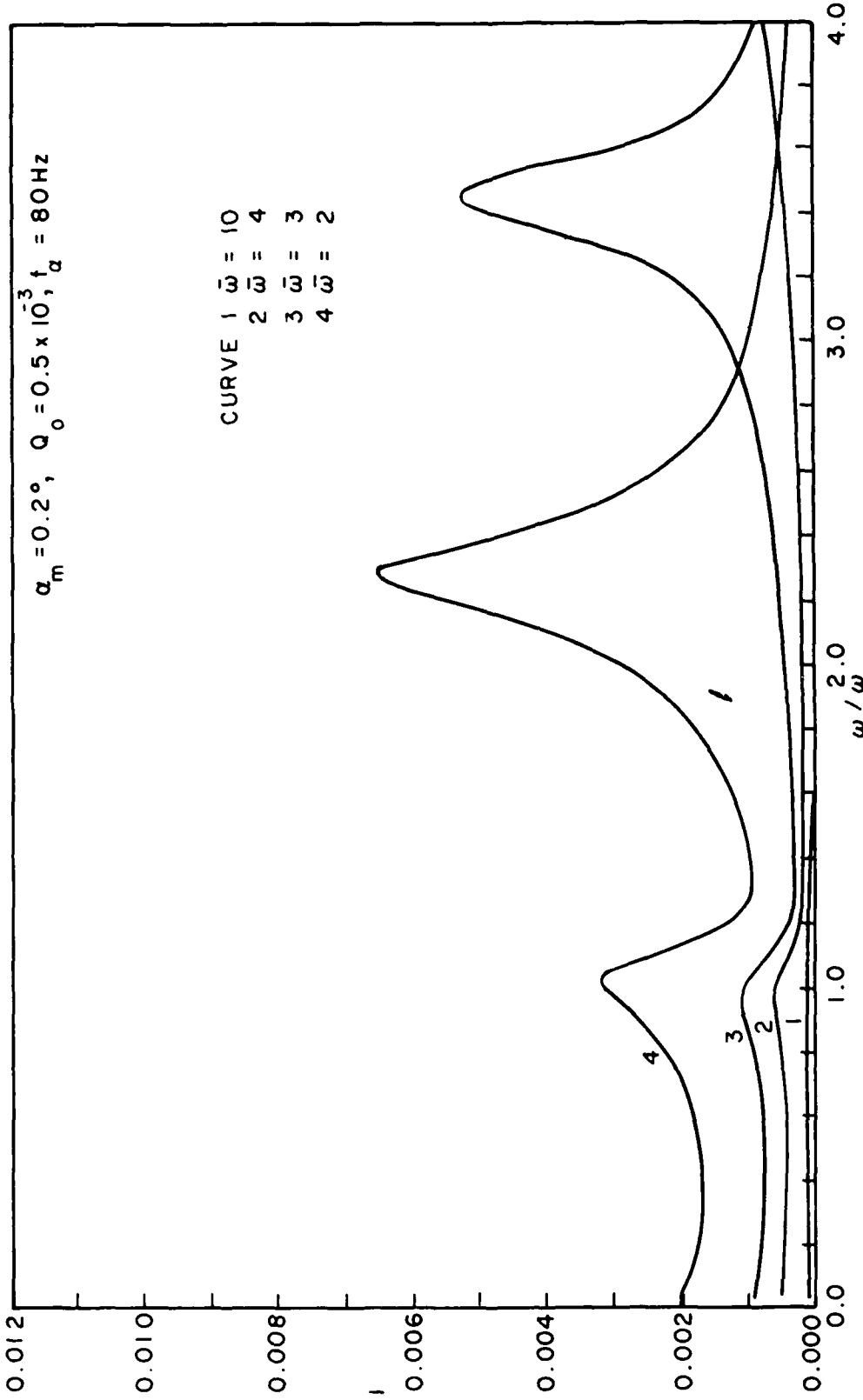

FIG. 19: VARIATION OF THE AMPLITUDE OF ξ WITH ω/ω_α FOR AN AIRFOIL OSCILLATING IN PITCH AND PLUNGE, $\alpha_m = 0.2°$, $f_\alpha = 80$ Hz AND $Q_o = 0.5 \times 10^{-3}$

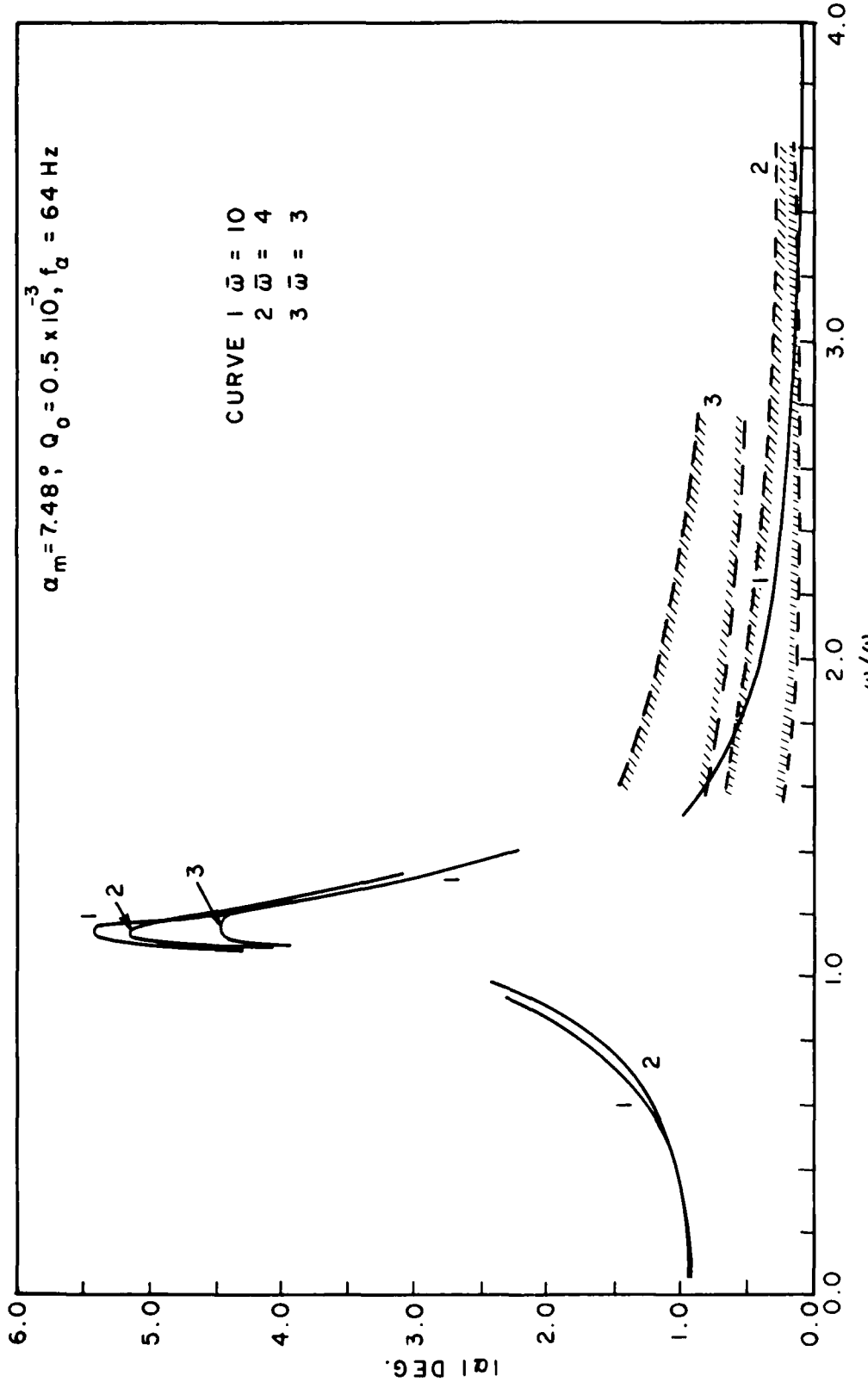

FIG. 20: VARIATION OF THE AMPLITUDE OF α WITH ω/ω_α FOR AN AIRFOIL OSCILLATING IN PITCH AND PLUNGE, α_m = 7.48°, f_α = 64 Hz AND Q_o = 0.5 × 10^{-3}

APPENDIX

The terms T and U on the RHS of Equations (20) and (21) and the coefficients E, V, M, I are given as:

$$T = r_{\tau+\Delta\tau} + B\alpha_{\tau} - C\alpha_{\tau-\Delta\tau} + D\alpha_{\tau-2\Delta\tau} + F\xi_{\tau} - G\xi_{\tau-\Delta\tau} + H\xi_{\tau-2\Delta\tau} \tag{A1}$$

$$U = p_{\tau+\Delta\tau} + N\xi_{\tau} - P\xi_{\tau-\Delta\tau} - S\xi_{\tau-2\Delta\tau} + J\alpha_{\tau} - K\alpha_{\tau-\Delta\tau} + L_{\tau-2\Delta\tau} \tag{A2}$$

where

$$r(\tau) = \frac{2}{\pi\mu r_{\alpha}^2} C_M(\tau) + \frac{Q(\tau)}{mU^2 r_{\alpha}^2}$$

$$p(\tau) = -\frac{1}{\pi\mu} C_N(\tau) + \frac{bP(\tau)}{mU^2}$$

$$B = \frac{5}{\Delta\tau^2} + \frac{6}{\Delta\tau}\frac{\zeta_{\alpha}}{U^*}$$

$$C = \frac{4}{\Delta\tau^2} + \frac{3}{\Delta\tau}\frac{\zeta_{\alpha}}{U^*}$$

$$D = \frac{1}{\Delta\tau^2} + \frac{2}{3\Delta\tau}\frac{\zeta_{\alpha}}{U^*}$$

$$F = \frac{5x_{\alpha}}{r_{\alpha}^2\Delta\tau^2}$$

$$G = \frac{4x_{\alpha}}{r_{\alpha}^2\Delta\tau^2}$$

$$H = \frac{x_{\alpha}}{r_{\alpha}^2\Delta\tau^2}$$

$$J = \frac{5x_{\alpha}}{\Delta\tau^2}$$

$$K = \frac{4x_\alpha}{\Delta\tau^2}$$

$$L = \frac{x_\alpha}{\Delta\tau^2}$$

$$N = \frac{5}{\Delta\tau^2} + \frac{6}{\Delta\tau}\zeta_\xi\frac{\bar{\omega}}{U^*}$$

$$P = \frac{4}{\Delta\tau^2} + \frac{3}{\Delta\tau}\zeta_\xi\frac{\bar{\omega}}{U^*}$$

$$S = \frac{1}{\Delta\tau^2} + \frac{2}{3\Delta\tau}\zeta_\xi\frac{\bar{\omega}}{U^*}$$

and

$$E = \frac{2x_\alpha}{r_\alpha^2\Delta\tau^2} \tag{A3}$$

$$V = \frac{2}{\Delta\tau^2} + \frac{11}{3\Delta\tau}\frac{\zeta_\alpha}{U^*} + \frac{1}{U^{*2}} \tag{A4}$$

$$M = \frac{2}{\Delta\tau^2} + \frac{11}{3\Delta\tau}\zeta_\xi\frac{\bar{\omega}}{U^*} + \frac{\bar{\omega}^2}{U^{*2}} \tag{A5}$$

$$I = \frac{2x_\alpha}{\Delta\tau^2} \tag{A6}$$

SUMMARY

Forced oscillation of a two-dimensional airfoil with attached and separated flows is investigated using nonlinear unsteady aerodynamics for pitching motion derived from a time synthesization technique utilizing oscillatory loop data determined experimentally. Both one- and two-degree-of-freedom oscillations are considered. The structural dynamic equations of motion are integrated by a time marching finite difference scheme. The airfoil response is examined for different values of spring stiffness and magnitudes of externally applied moment. For two-degree-of-freedom vibration, only small plunge amplitude is considered and the aerodynamic loads are approximated by the superposition of nonlinear terms due to pitch and linear terms due to plunge. The presence of a small amplitude plunging motion increases the pitch amplitude slightly for attached flow, while a decrease in pitch amplitude is predicted for separated flow.

RÉSUMÉ

On examine l'oscillation forcée d'un profil de voilure bidimensionel dans des écoulements de contact et séparé à partir de données d'aérodynamique non linéaire instable sur le mouvement de tangage produites par une technique de synthétisation du temps basée sur une boucle oscillatoire établie expérimentalement. On étudie les oscillations à un et à deux degrés de liberté. Les équations dynamiques structurales du mouvement sont intégrées par une méthode d'avancement du temps aux différences finies. La réponse du profil est examinée pour différentes valeurs de raideur d'un ressort et de moment externe. Pour les vibrations à deux degrés de liberté, seule l'amplitude des faibles plongeons est considérée et les charges aérodynamiques sont approchées par la superposition de termes non linéaires de tangage et de termes linéaires de plongeon. La présence d'un mouvement de plongeon de faible amplitude augmente légèrement l'amplitude du tangage pour l'écoulement de contact, tandis qu'on prévoit une diminution de l'amplitude du tangage pour l'écoulement séparé.

END

DTIC

8-86